

Scale-Invariant Correspondence Analysis of Compositional Data

Choulakian V. & Allard J., Université de Moncton, Canada
 vartan.choulakian@umoncton.ca, jacques.allard@umoncton.ca

August 2025

Abstract

Correspondence analysis is a dimension reduction technique for visualizing a nonnegative matrix $\mathbf{N} = (n_{ij})$ of size $I \times J$, in particular contingency tables or compositional datasets; but it depends on the row and column marginals of \mathbf{N} . Three complementary transformations of the data $T(\mathbf{N}) = (T(a_i n_{ij} b_j))$ render CA of $T(\mathbf{N})$ invariant for any $a_i > 0$ and $b_j > 0$. First, Greenacre's scale-invariant approach, valid for positive data. Second, Goodman's marginal-free correspondence analysis, valid for positive or moderately sparse data. Third, correspondence analysis of the sign-transformed matrix, $\text{sign}(\mathbf{N}) = (\text{sign}(n_{ij}))$, valid for sparse or extremely sparse data. We demonstrate these three methods on four real-world datasets with varying levels of sparsity to compare their exploratory performance.

Key words: Scale-invariant correspondence analysis; Sinkhorn (RAS-ipf) algorithm; bistochastic matrix; log-linear association; sparsity indices; sign transformation.

AMS 2010 subject classifications: 62H25, 62H30

1 Overview of scale-invariant correspondence analysis

Correspondence analysis (CA) and log-ratio analysis (LRA) are two popular methods for the analysis and visualization of a two-way contingency table or compositional dataset $\mathbf{N} = (n_{ij})$ of size $I \times J$ for $i = 1, \dots, I$ and $j = 1, \dots, J$ and $n_{ij} \geq 0$.

LRA is considered theoretically ideal because it is invariant to arbitrary rescaling of rows and/or columns, making it fully scale-invariant. However, it requires strictly positive cell data (nonsparse $n_{ij} > 0$).

By contrast, CA can handle nonnegative cell data (sparse $n_{ij} \geq 0$) but lacks scale-invariance: its results depend on the marginal sums of rows and columns.

This paper develops a unified framework to render CA fully invariant under any row and column scalings—what Goodman (1996) called “marginal-free” CA—to place it on equal footing with the scale-invariant ideal of LRA. We present three data transformations $T(\mathbf{N}) = (T(a_i n_{ij} b_j))$ that guarantee CA on $T(\mathbf{N})$ is invariant for all positive scaling factors $a_i > 0$ and $b_j > 0$. Two of these transformations also convert the data into a bistochastic form.

1.1 Three Transformations to achieve scale-invariant CA

1) Limiting power (Box–Cox) transformation

Greenacre (2010, result 1) states that applying CA on $\mathbf{N}^{(\alpha)} = (n_{ij}^\alpha)$ for $\alpha \in (0, 1]$ seamlessly transitions to uniformly weighted LRA as $\alpha \rightarrow 0$. Greenacre’s approach is valid for strictly positive data, see section 3.

2) Sinkhorn (RAS-ipf) scaling

Scale rows and columns by positive factors $a_i > 0$ and $b_j > 0$ and iteratively adjust them to sum to one. This produces a unique bistochastic matrix. Goodman (1996) sketched a marginal-free CA by applying CA (mfCA) to this bistochastic table, accommodating positive to moderately sparse data, see section 4.

Goodman (1996)’s mfCA aims to marry Pearson-based CA with Yule’s ratio-based LRA for nonnegative data. As stated above, for positive data Greenacre’s limiting power-transform approach fully satisfies Goodman’s aim. Choulakian & Mahdi (2024) show mfCA is a special case of CA with pre-specified marginals, tracing back to Benzécri’s work.

3) Sign transformation

Replace every nonzero entry by 1, that is, apply $T(\mathbf{N}) = (\text{sign}(a_i n_{ij} b_j)) = (\text{sign}(n_{ij}))$. CA on this binary presence/absence table handles sparse or extremely sparse data that defeat other methods. It remains invariant to row and column rescalings but does not yield a bistochastic matrix, see section 6.

1.2 Bistochastic matrix

A nonnegative matrix $\mathbf{D} = (d_{ij})$ for $i = 1, \dots, I$ and $j = 1, \dots, J$, is named bistochastic (or doubly stochastic) if the following two conditions are satisfied: $\frac{1}{I} \sum_i d_{ij} = \frac{1}{J} \sum_j d_{ij} = 1$ for $i = 1, \dots, I$ and $j = 1, \dots, J$; see among others, Marshall et al. (2009, chapter 2) and Loukaki (2023). It follows that $\sum_{i,j} d_{ij} =$

IJ . So $\mathbf{Q} = \mathbf{D}/(IJ)$ is a probability measure with uniform marginals; that is, $\frac{1}{J} = q_{+j} = \sum_i q_{ij}$ and $\frac{1}{I} = q_{i+} = \sum_j q_{ij}$; Mosteller (1968) and Goodman (1996, Eq (39) and (40)) named \mathbf{Q} "the standardized distribution". So the concepts of doubly stochastic matrix \mathbf{D} and its associated probability measure $\mathbf{Q} = \mathbf{D}/(IJ)$ with uniform marginal weights are equivalent for nonnegative datasets.

According to Goodman (1996, section 6), the first step for mfCA is to transform the contingency table $\mathbf{N} = (n_{ij})$ into a bistochastic matrix \mathbf{D} by row and column scalings, where $\mathbf{D} = (d_{ij} = a_i n_{ij} b_j)$, $a_i > 0$ and $b_j > 0$ for $i = 1, \dots, I$ and $j = 1, \dots, J$. Row and column scalings of a matrix consists of pre- and post-multiplying the original matrix $\mathbf{N} = (n_{ij})$ by two diagonal matrices $Diag(a_i)$ and $Diag(b_j)$. The computational tool to achieve this will be the Sinkhorn algorithm, also known as the RAS method or the iterative proportional fitting (ipf) procedure; for a comprehensive survey see Idel (2016).

1.3 Contents

In our opinion, the study of row and column scale-invariant CA of a dataset \mathbf{N} emerges in two distinct situations depending on the sparsity of \mathbf{N} :

a) \mathbf{N} is *positive*, that is nonsparse ($n_{ij} > 0$), thus scalable to a unique bistochastic matrix by two different transformations. First, by a limiting power (similar to Box-Cox) transformation, which is equivalent to the uniformly weighted LRA association index by Greenacre (2010, Result 1)'s Theorem. Second, by row and column scalings by Sinkhorn (1964)'s algorithm implicitly suggested by Goodman (1996, Eq (39)). Both Greenacre and Goodman approaches are related: Goodman approach is a specific first-order approximation of Greenacre approach via uniformly weighted LRA.

b) \mathbf{N} is *nonnegative* (*there is at least one zero cell*). Here we can have two cases. Case 1) \mathbf{N} is scalable to a unique bistochastic matrix \mathbf{D} . This case is described by Goodman (1996, Eq (39)) and CA of \mathbf{D} is named mfCA. Case 2: \mathbf{N} is scalable to a matrix \mathbf{D} having the structure of multiple diagonal bistochastic blocks. We name CA of \mathbf{D} multiple mfCA. For extremely sparse data sets multiple mfCA is not valid; so we propose CA of sign transformed data, known also as binary (0/1 or presence/absence) data.

This paper is organized as follows: Section 2 presents preliminaries concerning CA and LRA association indices and their relationships with the additive and multiplicative double centering; section 3 discusses Greenacre's Theorem; section 4 presents Goodman's mfCA (cases 1 and 2); section 5 presents Sinkhorn (RAS-ipf) algorithm; section 6 compares the three scale-

invariant transformations, plus the row transformation based on Benzécri's homogeneity principle; section 7 presents four case studies; and we conclude in section 8.

Benzécri (1973a, b) is the reference book on CA but difficult to read because of his use of tensor notation. Among others, Greenacre (1984), Le Roux and Rouanet (2004) and Murtagh (2005) are the best representatives of Benzécri's approach; Beh and Lombardo (2014) present a panoramic review of CA. Taxicab CA (TCA) is a robust variant of CA which will be also used in this paper; see in particular Choulakian (2006, 2016) and Choulakian, Allard and Mahdi (2023).

2 Preliminaries on the analysis of contingency tables

We consider a two-way contingency table $\mathbf{N} = (n_{ij})$ for $i = 1, \dots, I$ and $j = 1, \dots, J$, and $\mathbf{P} = \mathbf{N}/n = (p_{ij})$ of size $I \times J$ the associated correspondence matrix (probability table) of the contingency table \mathbf{N} . We define as usual $p_{i+} = \sum_{j=1}^J p_{ij}$, $p_{+j} = \sum_{i=1}^I p_{ij}$, the vector $(p_{i+}) \in \mathbb{R}^I$, the vector $(p_{+j}) \in \mathbb{R}^J$, and $\mathbf{M}_I = \text{Diag}(p_{i+})$ the diagonal matrix having diagonal elements p_{i+} , and similarly $\mathbf{M}_J = \text{Diag}(p_{+j})$. We suppose that \mathbf{M}_I and \mathbf{M}_J are positive definite metric matrices of size $I \times I$ and $J \times J$, respectively; this means that the diagonal elements of \mathbf{M}_I and \mathbf{M}_J are strictly positive.

First, we review the CA and LRA association indices, then double centering of a dataset.

2.1 Association indices

The CA association index of a probability table \mathbf{P} is

$$\Delta_{ij}(\mathbf{P}) = \frac{p_{ij}}{p_{i+}p_{+j}} - 1, \quad (1)$$

where $\frac{p_{ij}}{p_{i+}p_{+j}}$ is named the density function of p_{ij} with respect to the product measure $p_{i+}p_{+j}$.

Assuming $p_{ij} > 0$, we define the LRA association index (named log-linear association index by Goodman (1996) with uniform weights to be

$$\lambda(p_{ij}, w_i^R = 1/I, w_j^C = 1/J) = \log(p_{ij}) + \frac{1}{IJ} \sum_{i,j} \log(p_{ij}) - \left(\frac{1}{I} \sum_i \log(p_{i+}) + \frac{1}{J} \sum_j \log(p_{+j}) \right). \quad (2)$$

Equation (2) appears also in compositional data analysis, see Aitchison (1986), and in spectral mapping of Lewi (1976).

2.2 Scale-invariance

The CA association index (1) depends on the table's marginal distributions and will shift if you change any row or column sum, whereas the LRA association index (2) is unaffected by any positive rescaling of rows or columns, that we describe. Let $\tau_{ij}(p_{ij})$ represent an interaction (association) index, such as $\Delta_{ij}(\mathbf{P})$ or $\lambda(p_{ij}, w_i^R = 1/I, w_j^C = 1/J)$ described in equations (1) and (2) respectively. Following Yule (1912) and Goodman (1996), we state the following

Definition 1: An interaction index $\tau_{ij}(p_{ij} = \frac{n_{ij}}{\sum_{i,j} n_{ij}})$ is scale-invariant if $\tau_{ij}(p_{ij}) = \tau_{ij}(q_{ij} = \frac{a_i n_{ij} b_j}{\sum_{i,j} a_i n_{ij} b_j})$ for arbitrary positive scales $a_i > 0$ and $b_j > 0$.

The CA index $= \frac{p_{ij}}{p_{i+}p_{+j}} - 1$ fails this property. Lemma 1 generalizes

$$\lambda\left(\frac{p_{ij}}{p_{i+}p_{+j}}, w_i^R = p_{i+}, w_j^C = p_{+j}\right) = \lambda(p_{ij}, w_i^R = p_{i+}, w_j^C = p_{+j})$$

stated in Goodman (1996).

Lemma 1

a) The LRA association index (3) with prespecified positive weights (w_i^R, w_j^C)

$$\lambda(p_{ij}, w_i^R, w_j^C) = \log(p_{ij}) + \sum_{i,j} w_i^R w_j^C \log(p_{ij}) - \left(\sum_i w_i^R \log(p_{ij}) + \sum_j w_j^C \log(p_{ij}) \right) \quad (3)$$

is scale-invariant. In particular the LRA association index (2) with uniform weights is scale-invariant.

b) The first-order approximation of (3) is

$$\lambda(p_{ij}, w_i^R, w_j^C) \approx \frac{p_{ij}}{w_i^R w_j^C} - \frac{p_{i+}}{w_i^R} - \frac{p_{+j}}{w_j^C} + 1.$$

For a proof see Choulakian, Allard and Mahdi (2023).

Remarks:

a) A result stated in Cuadras, Cuadras, and Greenacre (2006) is

$$\lambda(p_{ij}, w_i^R = p_{i+}, w_j^C = p_{+j}) \approx \Delta_{ij}(\mathbf{P}) = \frac{p_{ij}}{p_{i+}p_{+j}} - 1.$$

b) We emphasize the fact that in general

$$\lambda(p_{ij}, w_i^R = 1/I, w_j^C = 1/J) \approx IJp_{ij} - Ip_{i+} - Jp_{+j} + 1,$$

is *not related* to CA association index $\Delta_{ij}(\mathbf{P})$, unless \mathbf{P} is bistochastic, and in this particular case Goodman's mfCA association index is a specific first-order approximation of Greenacre's scale-invariant CA association index via Lemma 1b, see subsection 4.1.

2.3 Double centering

Both the CA association index $\Delta_{ij}(\mathbf{P})$ and the LRA association index $\lambda(p_{ij}, w_i^R = 1/I, w_j^C = 1/J)$ are double centered; that is:

$$\begin{aligned} 0 &= \sum_{i=1}^I p_{i+} \Delta_{ij}(\mathbf{P}) = \sum_{i=1}^I \frac{1}{I} \lambda(p_{ij}, w_i^R = 1/I, w_j^C = 1/J) \\ &= \sum_{j=1}^J p_{+j} \Delta_{ij}(\mathbf{P}) = \sum_{j=1}^J \frac{1}{J} \lambda(p_{ij}, w_i^R = 1/I, w_j^C = 1/J). \end{aligned} \quad (4)$$

According to Tukey (1977, chapter 10), there are two kinds of double centering that he named *row-PLUS-column* and *row-TIMES-column*; we name them *additive* and *multiplicative*, that we describe.

More generally, let $y_{ij} = h(p_{ij})$ be any transform of p_{ij} , and define the three weighted means $Y_{i+} = \sum_{j=1}^J y_{ij} w_j^C$, $Y_{+j} = \sum_{i=1}^I y_{ij} w_i^R$ and $Y_{++} = \sum_{j=1}^J \sum_{i=1}^I y_{ij} w_i^R w_j^C$. Two centering schemes arise:

a) Multiplicative (row-times-column):

$$\tau_{ij} = y_{ij} - \frac{Y_{i+} Y_{+j}}{Y_{++}}, \quad (5)$$

where $\text{rank}(\tau_{ij}) = \text{rank}(y_{ij}) - 1$.

b) Additive (row-plus-column):

$$\tau_{ij} = y_{ij} + Y_{++} - (Y_{i+} + Y_{+j}), \quad (6)$$

where $\text{rank}(\tau_{ij}) = \text{rank}(y_{ij}) - 1$ or $\text{rank}(y_{ij}) - 2$.

Only the additive version is invariant to adding a constant a_i to the i th row or b_j to the j th column of (y_{ij}) : Thus Lemma 1 becomes a corollary to this fact.

We consider two functional forms of $y_{ij} = h(p_{ij})$.

a) $y_{ij} = h(p_{ij}) = \log p_{ij}$ for $p_{ij} > 0$. First, the log-linear interaction $\tau_{ij} = \lambda(p_{ij}, w_i^R, w_j^C)$ is obtained from (6). So the rank $(\lambda(p_{ij}, w_i^R, w_j^C)) = \text{rank}(\log p_{ij}) - 1$, as in Goodman (1991, Table 11); or rank $(\lambda(p_{ij}, w_i^R, w_j^C)) = \text{rank}(\log p_{ij}) - 2$, as in Goodman (1991, Table 10). Second, to our knowledge the log-interaction obtained from (5) has not been applied yet, most probably due to the fact that it is not row and column scale-invariant.

b) $y_{ij} = h(p_{ij}) = \frac{p_{ij}}{w_i^R w_j^C}$ is the density function of the joint probability measure p_{ij} with respect to the product measure $w_i^R w_j^C$. The CA interaction $(\tau_{ij}) = (\Delta_{ij}(\mathbf{P}))$ is obtained either from (5) or from (6), when $(w_i^R, w_j^C) = (p_{i+}, p_{+j})$. So the rank $(\Delta_{ij}(\mathbf{P})) = \text{rank}(\frac{p_{ij}}{p_{i+} p_{+j}}) - 1$. This property of CA seems *unique*. So we ask the following question: Under what condition the additive double centering equals the multiplicative double centering, (5) = (6)? The proof of the next lemma is easy.

Lemma 2: Assuming $y_{ij} \geq 0$, equations (5) = (6) = $y_{ij} - Y_{++}$ if and only if $Y_{++} = Y_{i+} = Y_{+j}$ for $i = 1, \dots, I$ and $j = 1, \dots, J$.

Corollary 1:

a) In CA, taking $y_{ij} = \frac{p_{ij}}{p_{i+} p_{+j}}$ give all three marginals equal to 1:

$$Y_{i+} = \sum_j p_{+j} \frac{p_{ij}}{p_{i+} p_{+j}} = Y_{++} = \sum_{i,j} p_{i+} p_{+j} \frac{p_{ij}}{p_{i+} p_{+j}} = Y_{+j} = 1;$$

so both centering schemes produce $\Delta_{ij}(\mathbf{P}) = \frac{p_{ij}}{p_{i+} p_{+j}} - 1$; see also Goodman (1996, Eq (11)).

b) If \mathbf{Y} is any bistochastic matrix, then it too has uniform marginals, making the two centering formulas identical for $y_{ij} = IJ p_{ij}$.

2.4 Underlying structure via CA

Following Benzécri (1973b, p.6)'s famous second principle '*Le modèle doit suivre les données, non l'inverse*', "the model must follow the data, not the inverse", one can read off the underlying structure of a data set from CA (or TCA) outputs such as figures or dispersion values, see in particular Benzécri (1973b, pp.43-46 and pp. 188-195) and Benzécri (1973a, pp. 261-287).

The following two results are well known for sparse datasets \mathbf{N} :

Theorem (Benzécri (1973b, pp188-190)) If the first $m < \text{rank}(\mathbf{P}) - 1$ singular values of CA of \mathbf{P} all equal 1, $\rho_\alpha = 1$ for $\alpha = 1, \dots, m$, then the latent underlying structure of the contingency table \mathbf{N} decomposes into $(m + 1)$ independent blocks, and CA reduces to separate analyses of each block.

Remark 1: Benzécri (1973b, p.189-190) observed that it is rare to have $\rho_1 = 1$, but not uncommon to have $\rho_1^2 \geq 0.7$ or $\rho_1 \geq 0.837$; then the underlying structure of the contingency table may be either quasi-2 blocks diagonal or band diagonal.

2.5 Sparsity indices in CA

Given $\mathbf{N} = (n_{ij})$ of size $I \times J$ three indices of sparsity (in % or proportion of zero cells $n_{ij} = 0$) are defined within CA framework, for the first two see Choulakian (2017):

a) **Apparent sparsity** of (\mathbf{N}) in % = $100 \frac{\text{number of } (n_{ij}=0)}{IJ}$.

b) Compute $\mathbf{N}_{merged} = (n_{ij}^*)$ of size $I_1 \times J_1$, where $I_1 \leq I$ and $J_1 \leq J$, by combining rows and columns of \mathbf{N} which are proportional. Note that CA (or TCA) of \mathbf{N} is equivalent (identical) to CA (or TCA) of \mathbf{N}_{merged} based on Benzécri's principle of distributional equivalence. Then

$$\begin{aligned} \text{CA sparsity of } (\mathbf{N}) &= \text{Apparent sparsity of } (\mathbf{N}_{merged}) \\ &= \frac{\text{number of } (n_{ij}^* = 0)}{I_1 J_1}. \end{aligned}$$

c) According to Loukaki (2023, Theorem 1) the sparsest nonnegative bistochastic matrix \mathbf{S} of size $I_1 \times J_1$ has the smallest support (number of positive cells) of $S(I_1, J_1) = I_1 + J_1 - \gcd(I_1, J_1)$; so

$$\text{sparsity of } (\mathbf{S}) = \frac{I_1 J_1 - S(I_1, J_1)}{I_1 J_1}.$$

Define

$$\text{Adjusted sparsity of } (\mathbf{N}) = \frac{\text{CA sparsity of } (\mathbf{N})}{\text{sparsity of } (\mathbf{S} \text{ of size } I_1 \times J_1)}.$$

Note that the sparsest bistochastic square matrices \mathbf{S} are diagonal with sparsity index of $(1 - 1/I_1)$.

Example 1: Let

$$\mathbf{N} = \begin{bmatrix} 1 & 1 & 1 & 1 & 1 \\ 1 & 1 & 0 & 0 & 1 \\ 1 & 1 & 0 & 0 & 1 \\ 1 & 1 & 1 & 1 & 1 \\ 1 & 1 & 1 & 1 & 1 \\ 1 & 1 & 1 & 1 & 1 \end{bmatrix};$$

By Benzécri's principle of distributional equivalence, it is CA equivalent to

$$\mathbf{N}_{merged} = \begin{bmatrix} 12 & 8 \\ 6 & 0 \end{bmatrix}$$

So: apparent sparsity of $(\mathbf{N}) = 4/30$, CA sparsity of $(\mathbf{N}) = 1/4$, and adjusted sparsity of $(\mathbf{N}) = 1/2$.

3 Greenacre's Theorem

Greenacre's Theorem equates both CA and LRA association indices in a very simple way (that is, equations (1) = (2)): Let $\mathbf{P}^{(\alpha)} = (p_{ij}^{(\alpha)} = \frac{n_{ij}^{(\alpha)}}{\sum_{i,j} n_{ij}^{(\alpha)}})$ for $i = 1, \dots, I$ and $j = 1, \dots, J$ be the correspondence table of the simple power transformed data, $p_{i+}^{(\alpha)} = \sum_j p_{ij}^{(\alpha)}$ and $p_{+j}^{(\alpha)} = \sum_i p_{ij}^{(\alpha)}$ for $\alpha > 0$. We consider the CA association index

$$\Delta_{ij}(\mathbf{P}^{(\alpha)}) = \frac{p_{ij}^{(\alpha)} - p_{i+}^{(\alpha)} p_{+j}^{(\alpha)}}{p_{i+}^{(\alpha)} p_{+j}^{(\alpha)}}. \quad (7)$$

Then, Choulakian (2023) and Greenacre (2024) proved the following result:

Greenacre's Theorem (Greenacre (2010, Result 1)

Under the assumption $n_{ij} > 0$, for $\alpha \rightarrow 0$ and $\alpha > 0$

$$\begin{aligned} \lim_{\alpha \rightarrow 0} \frac{\Delta_{ij}(\mathbf{P}^{(\alpha)})}{\alpha} &= \lim_{\alpha \rightarrow 0} \left(\frac{p_{ij}^{(\alpha)}}{p_{i+}^{(\alpha)} p_{+j}^{(\alpha)}} - 1 \right) / \alpha \\ &= \lambda(p_{ij}, w_i^R = 1/I, w_j^C = 1/J), \text{ and by Lemma 1a} \\ &= \lambda(q_{ij} = a_i p_{ij} b_j, w_i^R = 1/I, w_j^C = 1/J) \text{ for } a_i, b_j > 0 \quad (8) \\ &= \lim_{\alpha \rightarrow 0} \frac{\Delta_{ij}(\mathbf{Q}^{(\alpha)})}{\alpha}. \end{aligned}$$

Moreover, the row and column margins of both $\mathbf{P}^{(\alpha)}$ and $\mathbf{Q}^{(\alpha)}$ become uniform:

$$\lim_{\alpha \rightarrow 0} p_{i+}^{(\alpha)} = \lim_{\alpha \rightarrow 0} q_{i+}^{(\alpha)} = 1/I \text{ for } i = 1, \dots, I \text{ and } \lim_{\alpha \rightarrow 0} p_{+j}^{(\alpha)} = \lim_{\alpha \rightarrow 0} q_{+j}^{(\alpha)} = 1/J \text{ for } j = 1, \dots, J. \quad (9)$$

Remark 2: There are two important aspects in Greenacre's Theorem that we want to emphasize.

- a) It shows the conditions under which CA becomes row and column scale-invariant, equation (8).
- b) It implies that the row and column marginals of $\mathbf{P}^{(\alpha)}$ for $\alpha > 0$ and $\alpha \simeq 0$ are almost uniform, equation (9); so $\mathbf{P}^{(\alpha)}$ is bistochastic.

3.1 CA decomposition

The limit association (8) can be decomposed as

$$\begin{aligned}\lambda(p_{ij}, w_i^R = 1/I, w_j^C = 1/J) &= \lim_{\alpha \rightarrow 0} \frac{\Delta_{ij}(\mathbf{P}^{(\alpha)})}{\alpha} \\ &= \sum_{m=1}^M \mu_{im} \nu_{jm} \rho_m,\end{aligned}$$

where $M = \text{rank}(\mathbf{P}) - 1$ and the parameters $(\mu_{im}, \nu_{jm}, \rho_m)$ satisfy, for $s, m = 1, \dots, M$

$$\begin{aligned}1 &= \sum_{i=1}^I \mu_{im}^2 / I = \sum_{j=1}^J \nu_{jm}^2 / J \\ 0 &= \sum_{i=1}^I \mu_{im} / I = \sum_{j=1}^J \nu_{jm} / J \\ 0 &= \sum_{i=1}^I \mu_{im} \mu_{is} / I = \sum_{j=1}^J \nu_{jm} \nu_{js} / J \quad \text{for } m \neq s.\end{aligned}$$

The parameter $\rho_m \in (0, 1]$ admits two interpretations:

First, $\rho_m = \text{corr}(\mu_{mi}, \nu_{mj}) = \sum_{i,j} \mu_{mi} \nu_{mj} p_{ij}$ is the Pearson correlation coefficient of the m th principal dimension row and column scores (μ_{mi}, ν_{mj}) within the framework of CA of $\mathbf{P}^{(\alpha)}$.

Second, it represents the uniformly weighted intrinsic association within the framework of Goodman (1991, Eq. 3.7)'s RC association model, which can be expressed as a function of log-odds ratio

$$\begin{aligned}\log\left(\frac{p_{ij} p_{i_1 j_1}}{p_{ij_1} p_{i_1 j}}\right) &= \sum_{m=1}^M (\mu_{im} - \mu_{i_1 m})(\nu_{jm} - \nu_{j_1 m}) \rho_m \\ &= \lim_{\alpha \rightarrow 0} \frac{\Delta_{ij}(\mathbf{P}^{(\alpha)}) + \Delta_{i_1 j_1}(\mathbf{P}^{(\alpha)}) - \Delta_{i_1 j}(\mathbf{P}^{(\alpha)}) - \Delta_{i j_1}(\mathbf{P}^{(\alpha)})}{\alpha}.\end{aligned}$$

The last relation is called tetra differences by Rao (1973, p.12); and it perfectly reconciles Pearson correlation measure ρ_m with Yule's log-odds ratio measure, an effort attempted by Mosteller (1968) and by Goodman (1996, section 10).

4 Goodman's mfCA and Sinkhorn scaling

In Greenacre's Theorem, the strict positivity assumption ($p_{ij} > 0$) is essential and there is only one parameter α . Here, we relax that assumption to nonnegativity ($p_{ij} \geq 0$) and introduce $(I+J)$ scaling parameters to transform the matrix $\mathbf{P} = (p_{ij})$ into a nonnegative bistochastic matrix $\mathbf{Q} = (q_{ij} = a_i p_{ij} b_j)$ using Sinkhorn (1964)'s algorithm—also known as the RAS algorithm or the iterative proportional fitting (ipf) procedure. Depending on the arrangement of zeros in \mathbf{P} , two distinct cases arise, characterized by Sinkhorn and Knopp (1967) and independently by Brualdi et al. (1966) as *fully indecomposable* and *reducible*. As we will see in the applications, the sparsity pattern of the original data plays a fundamental role.

4.1 Case 1: Nonsparse or moderately sparse fully indecomposable matrices

When the dataset \mathbf{N} is either strictly positive (nonsparse $n_{ij} > 0$) or nonnegative with a fully indecomposable structure (i.e., there exists a perfect matching along a permutation of rows and columns), there is a unique choice of positive scaling elements $a_i, b_j, \varphi_i, \psi_j > 0$ such that

$\mathbf{Q} = (q_{ij}) = (a_i p_{ij} b_j) = (\varphi_i n_{ij} \psi_j)$ is unique and bistochastic:

$$\mathbf{Q} = (q_{ij} = a_i p_{ij} b_j) \text{ such that } q_{i+} = 1/I \text{ and } q_{+j} = 1/J \quad (10)$$

Sinkhorn (1964) established this result for positive matrices, and Sinkhorn & Knopp (1967) along with Brualdi et al. (1966) extended it to nonnegative, fully indecomposable matrices (with further examples for rectangular arrays given by Loukaki (2023)).

For the resulting bistochastic matrix \mathbf{Q} , Goodman's mfCA association index is defined as

$$\Delta_{ij}(\mathbf{Q}) = IJq_{ij} - 1. \quad (11)$$

Remark: For strictly positive (nonsparse $n_{ij} > 0$) data, Goodman's mfCA association index (11) is a first-order approximation of Greenacre's

scale-invariant CA association index

$$\begin{aligned}
\lim_{\alpha \rightarrow 0} \frac{\Delta_{ij}(\mathbf{P}^{(\alpha)})}{\alpha} &= \lambda(p_{ij}, w_i^R = 1/I, w_j^C = 1/J), \text{ by Lemma 1a} \\
&= \lambda(q_{ij} = a_i p_{ij} b_j, w_i^R = 1/I = q_{i+}, w_j^C = 1/J = q_{+j}) \text{ for } a_i, b_j > 0 \\
&\approx \Delta_{ij}(\mathbf{Q}) = IJ q_{ij} - 1 \text{ by Lemma 1b.}
\end{aligned}$$

4.2 Case 2: Sparse or extremely sparse reducible matrices

When \mathbf{P} (or \mathbf{N}) exhibits a high degree of sparsity and its nonzero entries cluster into k disjoint blocks, the Sinkhorn (RAS-ipf) procedure yields block-wise scaling rather than a unique global solution. In this reducible case, one obtains scaling elements $a_{i\beta}^*, b_{j\beta}^* > 0$ for each block $\beta = 1, \dots, k$, producing a block-diagonal matrix

$$\begin{aligned}
\mathbf{Q}^* &= (q_{\beta(ij)}^* = a_{i\beta}^* p_{ij} b_{j\beta}^*) \\
&= \text{Diag}(\mathbf{B}_1 \dots \mathbf{B}_\beta \dots \mathbf{B}_k)', \tag{12}
\end{aligned}$$

where each submatrix \mathbf{B}_β is itself bistochastic but may have different uniform marginals. By Benzécri's Theorem (see subsection 2.3), CA of \mathbf{Q}^* is equivalent to k CA of \mathbf{B}_β for $\beta = 1, \dots, k$.

The corresponding block-specific mfCA index takes the form

$$\Delta_{ij}(\mathbf{P}, a_{i\beta}^*, b_{j\beta}^*) = \frac{a_{i\beta}^* p_{ij} b_{j\beta}^*}{c_\beta r_\beta} - 1, \tag{13}$$

where the terms $c_\beta, r_\beta > 0$ represent different uniform marginals of the blocks $\beta = 1, \dots, k$.

Example 2: The following simple 2 blocks diagonal dataset is sparse reducible

$$\begin{aligned}
\mathbf{N} &= \begin{bmatrix} \mathbf{B}_1 & 0 \\ 0 & \mathbf{B}_2 \end{bmatrix} \\
&= \begin{bmatrix} 1 & 1 & 1 & 0 \\ 0 & 0 & 0 & 1 \\ 0 & 0 & 0 & 1 \end{bmatrix}.
\end{aligned}$$

Each of the 2 blocks $\mathbf{B}_1 = (1 \ 1 \ 1)$ and $\mathbf{B}_2' = (1 \ 1)$ is bistochastic. However, because there is no way to mix entries across the two blocks, the overall matrix cannot be made globally bistochastic. Instead, we treat it as two separate bistochastic blocks under the reducible case.

5 The Sinkhorn (RAS-ipf) algorithm

The Sinkhorn algorithm (also known as the RAS or iterative proportional fitting procedure) is a simple method for adjusting a contingency table so that its row and column margins match prespecified targets. Because the literature on this topic is extensive, we refer readers to Idel (2016) for a comprehensive survey.

As Madre (1980) explains, there are three variants of this algorithm:

- Two variants alternate between scaling the row sums and scaling the column sums (this alternating-update approach is the standard and most widely studied; see, for example, Landa et al. (2022), Algorithm 2).
 - The third variant updates both row and column marginals simultaneously.
- In this paper—and in the R code provided below—we adopt the simultaneous-update variant.

To assess convergence, we employ two criteria that a bistochastic matrix $\mathbf{D} = (d_{ij})$ must satisfy (see Subsection 1.2 and Corollary 1b).

- 1) **C2dist**, which measures the deviation of the average row and column sums from their target of 1:

$$C2_{dist} = \sum_{i,j} \left| \left(\frac{1}{I} \sum_i d_{ij} + \frac{1}{J} \sum_j d_{ij} \right) - 2 \right|,$$

- 2) **ratio**, which compares the total mass of \mathbf{D} to the ideal mass IJ :

$$ratio = \sum_{i,j} d_{ij} / IJ.$$

If \mathbf{D} is bistochastic, then $C2_{dist} = 0$ and $ratio = 1$. The following R code is used in the applications.

```
# alg3 Madre Simultaneous adjustments
nRow <- nrow(dataMatrix)
nCol <- ncol(dataMatrix)
rowPrUnif <- rep(1/nRow, nRow)
colPrUnif <- rep(1/nCol, nCol)
nit <- 500      # nit = number of iterations
qij <- dataMatrix/sum(dataMatrix)
for (jj in 1:nit) {
  rowPROBA <- apply(qij,1,sum)
  colPROBA <- apply(qij,2,sum)
  dij <- qij/(rowPROBA %*% t(colPROBA))
```

```

qij <- dij/sum(dij)
Gj <- t(rowPrUnif) %*% dij
Gi <- dij %*% colPrUnif
C2 <- ((rep(1, nRow) %*% Gj) +(Gi %*% t(rep(1, nCol)))-2
C2dist = sum(abs(C2))
ratio = sum(dij)/(nRow*nCol)
su = c(jj,C2dist,ratio)
print(su)
}

```

6 Data transformations

The main instigation of this paper is the bistochastic similarity of equations (9) and (10). In (9) there is one parameter $\alpha \approx 0$, while in (10) there are $(I + J)$ positive scaling parameters (a_i, b_j) . To understand the difference between (9) and (10), we introduce the concept of a transformation that does not change the internal order (cellwise) structure in a contingency table, and show that row and column scalings (Cases 1 and 2) in mfCA are transformations that may change dramatically the cellwise structure thus uncovering the local-micro level interactions among some rows and columns in mfCA.

Definition 2: A transformation T of a contingency table $\mathbf{N} = (n_{ij})$ keeps the *internal order structure* unchanged if it satisfies the following inequality:

$$n_{ij} \leq n_{i_1 j_1} \text{ then } T(n_{ij}) \leq T(n_{i_1 j_1}). \quad (14)$$

It is evident that the simple power transformation by $T(n_{ij}) = n_{ij}^\alpha$ for $\alpha > 0$ in Greenacre's Theorem satisfies (14); while the transformations in Cases 1 and 2 represented in equations (10) and (12) by $T(p_{ij}) = a_i p_{ij} b_j$ and $T(p_{ij}) = a_{i\beta}^* p_{ij} b_{j\beta}^*$ in general do not satisfy (14), as shown by the following simple contrived example.

Example 3 and its interpretation: We apply the Sinkhorn (RAS-ipf) algorithm to the following table, a variant first studied by Sinkhorn(1964),

$$\mathbf{N} = \begin{bmatrix} 0 & 2 \\ 1 & 30 \end{bmatrix}.$$

After $nit = 500$ iterations we get: $C2_{dist} = 4.128788e - 03 \simeq 0$, $ratio = 9.999990e - 01 \simeq 1$ and

$$T(\mathbf{N}) = \mathbf{D} = \begin{bmatrix} 0 & 1.9980667962 \\ 1.997934 & \epsilon_{nit=500} = 0.003995601 \end{bmatrix} \simeq \begin{bmatrix} 0 & 2 \\ 2 & 0 \end{bmatrix}$$

which does not satisfy (14) at 2 cells.

Let us interpret both tables \mathbf{N} and $T(\mathbf{N})$. In \mathbf{N} , row 2 and column 2 are intensely related for $n_{22} = 30$, thus exhibiting a global-macro level probability association; while in $T(\mathbf{N})$ we observe two local-micro level probability associations (row 2 and column 1) and (row 1 and column 2) which are independent.

6.1 Sign transformation

Define the sign transformation $T(n_{ij}) = sign(n_{ij})$, which is invariant under any positive row- and column-scalings

$$sign(n_{ij}) = sign(a_i n_{ij} b_j) \quad \text{for } a_i > 0 \text{ and } b_j > 0.$$

This transformation satisfies property (14) and encodes a uniform association between row i and column j :

- $sign(n_{ij}) = 1$ indicates presence of association,
- $sign(n_{ij}) = 0$ indicates absence of association.

This approach is especially valuable for sparse or extremely sparse matrices.

Moreover, recall that for any vector $\mathbf{x} \in R^p$, the l_0 -norm (which is not a norm!) $\|\mathbf{x}\|_0 = \lim_{\alpha \rightarrow 0} \sum_j |x_j|^\alpha$ counts the number of nonzero entries in \mathbf{x} . Thus, when we perform CA on $sign(\mathbf{N})$, the weight assigned to each row or column equals the l_0 -norm of that row or column.

The small data set above in Example 3 becomes

$$sign(\mathbf{N}) = \begin{bmatrix} 0 & 1 \\ 1 & 1 \end{bmatrix},$$

where all positive cellwise probabilities are equal.

Remarks:

a) For nonnegative compositional datasets, power transformation $T(n_{ij}) = n_{ij}^\alpha$ for $\alpha \in [0, 1]$ is termed α -transformation by Tsagris et al. (2011, 2023) and chiPower transformation by Greenacre (2024). Their approach

is row stochastic (RS): $p_{i+}^{(\alpha)} = 1/I$ for $i = 1, \dots, I$ where rows represent the samples, while the column marginals vary $\min_j(p_{+j}^{(\alpha)}) \leq p_{+j}^{(\alpha)} \leq \max_j(p_{+j}^{(\alpha)})$ for $j = 1, \dots, J$. In the next two paragraphs we discuss two particular cases $\alpha = 1$ and 0 .

b) Benzécri (1973b, pp. 18-27) emphasized the following fact: CA must be applied only to *homogenous* datasets; for a compositional dataset \mathbf{N} where the rows represent samples, homogeneity is obtained by eliminating the scale of each row, changing \mathbf{N} into a row stochastic matrix $\text{RS}(\mathbf{N}) = (n_{ij} / \sum_j n_{ij})$; this action is called *closure* within the framework of compositional data analysis. This case corresponds to $\alpha = 1$. The underlying idea of Benzécri's homogeneity principle is identical to Aitchison (1986)'s *coherence* principle for compositional data, because ratios of compositional parts (n_{ij} / n_{ij_1}) for $j \neq j_1$ or $n_{ij} / (\prod_j n_{ij})^{1/J}$ eliminate the i th row scale. Note that the pioneer of the Dutch school of data science, Jan de Leeuw, referred to Multiple Correspondence Analysis (MCA) as Homogeneity Analysis within the Gifi (1990) system.

c) We note that for sparse and extremely sparse data, the $\text{sign}(\mathbf{N})$ corresponds to $\alpha = 0$ but it is not row stochastic; so another variant for $\alpha = 0$ is to transform $\text{sign}(\mathbf{N})$ into a row stochastic matrix $\text{RS}(\text{sign}(\mathbf{N}))$.

7 Applications

We evaluate the three scale-invariant CA (and its robust L_1 variant TCA) methods by analyzing four data sets with different sparsity indices. For computations, we use the following two R packages: *ca* by Greenacre et al.(2022) and *TaxicabCA* by Allard and Choulakian (2019).

7.1 Cups dataset

The archaeological “Cups” compositional dataset \mathbf{N} comprises 47 observations by 11 variables, originally compiled by Baxter et al. (1990). Each of the 47 cups is described by the percentage by weight of 11 chemical elements. Greenacre and Lewi (2009) analyzed this dataset using log-ratio analysis (LRA), and it can be downloaded from the R package *easyCODA* (Greenacre 2020). Since every entry in the Cups dataset is strictly positive, Sinkhorn's (1964) theorem ensures that the Sinkhorn (RAS - ipf) algorithm converges to a unique solution.

Given the positivity of all cells, Figure 1 in Greenacre and Lewi (2009) presents the biplot from uniformly weighted LRA—also as Greenacre's scale-

invariant CA biplot—which is almost identical to the principal map (not shown) produced by Goodman’s mfCA. Below are the dispersion measures (nearly the same size) for both principal maps.

	ρ_1^2 (variance explained)	ρ_2^2 (variance explained)
Greenacre’s scale-invariant CA	$\rho_1^2 = 0.00833$ (39.6%)	$\rho_2^2 = 0.00638$ (30.0%)
Goodman’s mfCA	$\rho_1^2 = 0.0101$ (43.6%)	$\rho_2^2 = 0.00673$ (29.1%)

We just note that the transformation $\text{sign}(\mathbf{N})$ is senseless, because $\mathbf{N} = (n_{ij})$ is nonsparse, $n_{ij} > 0$.

Table 1: Sinkhorn (RAS-ipf) algorithm iteration results.

iteration	rodent		Copepods	
	$C2_{dist}$	ratio	$C2_{dist}$	ratio
491	302.96414	1.380883	1.98952e-13	1
492	257.13691	1.380883	2.819966e-13	1
493	302.96414	1.380883	1.98952e-13	1
494	257.13691	1.380883	2.819966e-13	1
495	302.96414	1.380883	1.98952e-13	1
496	257.13691	1.380883	2.819966e-13	1
497	302.96414	1.380883	1.98952e-13	1
498	257.13691	1.380883	2.819966e-13	1
499	302.96414	1.380883	1.98952e-13	1
500	257.13691	1.380883	2.819966e-13	1

7.2 Rodent ecological abundance dataset

We analyze a dataset of rodent abundances (\mathbf{N}) comprising 9 species observed in 28 California cities. Originally published by Bolger et al. (1997) and CA analyzed by Quinn and Keough (2002, p. 460, Figure 17.5). This dataset is available in the TaxicabCA R package (Allard & Choulakian, 2019).

The apparent sparsity of $(\mathbf{N}) = 66.27\%$; the size of \mathbf{N}_{merged} is 21×9 and the CA sparsity of $(\mathbf{N}) = 58.7\%$; $S(21, 9) = 21 + 9 - 3 = 27$, so the adjusted sparsity of $(\mathbf{N}) = 58.7/(1 - 27/(21 * 9)) = 68.48\%$.

Choulakian (2017) analyzed it by comparing the CA and TCA maps, and showed that it has quasi 2-blocks diagonal structure (or partly decomposable) as shown in Table 3 by Benzécri’s empirical criterion stated in Subsection 2.4, see $\text{ca}(\mathbf{N})\$sv$, $\text{ca}(\text{RS}(\mathbf{N}))\sv , $\text{ca}(\text{sign}(\mathbf{N}))\sv and $\text{ca}(\text{RS}(\text{sign}(\mathbf{N})))\sv , where RS means row stochastic:

	ρ_1	ρ_2	ρ_3	ρ_4	ρ_5	ρ_6
ca(\mathbf{N})\$sv	0.8639	0.6776	0.5362	0.3909	0.1889	0.1568
ca(RS(\mathbf{N}))\$sv	0.9554	0.8122	0.6211	0.5251	0.2009	0.1629
ca(sign(\mathbf{N}))\$sv	0.8167	0.5990	0.4458	0.4106	0.2605	0.2171
ca(RS(sign(\mathbf{N})))\$sv	0.8885	0.7704	0.5299	0.4795	0.3759	0.2622

7.2.1 CA of $sign(\mathbf{N})$

The close correspondence of dispersion values of $ca(\mathbf{N})$sv$ and $ca(sign(\mathbf{N}))$sv$ indicates that the principal maps (not shown) from CA on raw abundances and on their sign transformation are highly similar.

7.2.2 mfCA

Choulakian and Mahdi (2024) applied Goodman's mfCA and Taxicab mfCA (mfTCA) after using the ipfr R package (Ward & Macfarlane, 2020), which regularizes zeros by replacing them with a tiny positive constant to guarantee unique convergence of Sinkhorn's algorithm. In our approach, zeros remain unchanged, causing the Sinkhorn (RAS-ipf) algorithm to oscillate between two bistochastic solutions, see Table 1, when run for a fixed 500 iterations due to the underlying quasi 2-blocks diagonal structure (or partly decomposable) of \mathbf{N} . Both solutions produce the same four blocks but differ in their uniform row and column marginals, see Table 2. By Benzécri's Theorem 1, we validate convergence to the same four blocks by comparing CA singular values for the scaled matrix \mathbf{D} at iterations 499 and 500:

	ρ_1	ρ_2	ρ_3	ρ_4	ρ_5	ρ_6	ρ_7	ρ_8
iter = 500: $ca(\mathbf{D})$sv$	1	1	1	0.8052	0.7174	0.6336	0.4936	0.2558
iter = 499: $ca(\mathbf{D})$sv$	1	1	1	0.8052	0.7174	0.6336	0.4936	0.2558

Identical dispersion profiles at successive iterations provide a practical convergence check for large and sparse datasets.

The final scaled matrix \mathbf{D} decomposes into four blocks (Case 2), as displayed in Table 3. We proceed to interpret these blocks in terms of species-city associations.

Table 2: Row and column uniform marginals of 4 blocks of *rodent* data.

iteration 500 (499)		$C2_{dist} = 257.14 (302.96)$		
$100*colPROBA(c_\beta)$	36.23(4.76)	29.96(6.71)	5.25(13.13)	3.76(11.45)
columns	1	2	3,4,5,6,8	7,9
$100*rowPROBA(r_\beta)$	6.04(0.79)	4.28(0.96)	2.51(7.63)	2.19(5.47)
rows	24,21,17,	25,22,16,15	28,27,26,23	6,4,2
	14,10,9	11,8,7	20,19,18,13	12,5,3,1

Interpretation of Table 3 In Table 3, the array $\mathbf{T} = (t_{ij} = d_{ij\alpha}|\mathbf{n}_{ij})$, represents both matrices the original *rodent* contingency table $\mathbf{N} = (n_{ij})$ and the 4 bistochastic blocks $\mathbf{T}_\alpha = (d_{ij\alpha})$ for $\alpha = 1, 2, 3, 4$, where each bistochastic block is aligned on both left and right sides by double lines. For example,

$$\mathbf{T}_1 = (t_{ij} = d_{ij1}|\mathbf{n}_{ij}) = \begin{array}{|c|c|} \hline 1|1 \\ 1|3 \\ 1|2 \\ 1|1 \\ 1|3 \\ 1|1 \\ \hline \end{array}$$

which is of size 6×1 ; \mathbf{T}_2 is of size 7×1 ; \mathbf{T}_3 is of size 12×5 and \mathbf{T}_4 is of size 3×2 . A blank cell represents $(0|\mathbf{0})$, such as $t_{12} = (0|\mathbf{0})$.

The interpretation of \mathbf{T}_1 is: rodent 1 locally characterizes the sites (24, 1, 21, 10, 9, 14). Note that there is an observed count of 3 rodent 1s in the site 20, but rodent 1 does not locally characterize site 20; site 20 belongs to the third bistochastic block which is locally associated with the rodents (6, 8, 3, 5, 4). Similar interpretations also apply to the other three bistochastic matrices. So, the 4 bistochastic blocks can be considered as a classification of the abundance data set \mathbf{N} .

We also note the following: number of zero valued cells is 167 in \mathbf{N} (or in $\text{sign}(\mathbf{N})$); while the number of zeros is 196 in the scaled 4 blocks diagonal bistochastic submatrices in Table 3.

Table 3: 4 blocks diagonal bistochastic *rodent* abundance data.

sites	rod1	rod2	rod6	rod8	rod3	rod5	rod4	rod7	rod9
24	1 1								
17	1 3								
21	1 2	0 1							
10	1 1	0 2							
9	1 3	0 8							
14	1(1)	0 3							
7		1 11							
11		1 9							
15		1 11							
25		1 5							
22		1 3							
8		1 16							
16		1 4							
1		0 13	0.97 2		0.19 3	1.41 1	2.43 1		
20	0 3				2.09 27		2.91 1		
12		0 3	0.85 16	3.38 7	0.01 1	0.76 5			
3		0 4	2.30 9		1.22 36	1.48 2			
13		0 4	2.09 12		0.90 39	2.01 4			
28			0.68 1		0.91 10		3.41 1		
18		0 2	0.78 14	2.03 4	0.58 78	1.61 10			
5		0 2	0.50 16		0.26 63	0.99 11	3.26 21		
23			1.25 8	2.85 2		0.90 2			
26			1.71(11)	2.84(2)	0.45(22)				
27			0.88 9	0.90 1	0.38 29	2.84 10			
19					5 1				
6		0 1	0 8	0 2	0 48	0 12	0 35	1.65 12	0.35 2
2		0 1	0 16	0 2	0 57	0 9	0 65	1.35 8	0.65 3
4		0 4	0 30	0 18	0 53	0 5	0 1		2 3

7.3 Copepods dataset

We analyze the *Copepods* (sea insects) dataset \mathbf{N} of size 42×40 found in Greenacre's **CODAinPractice** website, which is analyzed by Graeve and Greenacre (2020). It comprises $I = 42$ specimens, each described by $J = 40$ fatty acids. Every specimen was captured in one of three seasons:

- Summer (s): 22 specimens
- Spring (sp): 12 specimens

- Winter (w): 8 specimens

The study's objective is to determine whether these fatty-acid profiles can distinguish among the three seasons.

7.3.1 Sparsity of the data

The dataset has an apparent sparsity (and CA sparsity) of 11.13%. Adjusted sparsity of 11.69% by using the formula $11.13/(1 - (42 + 40 - 2)/(42 * 40))$.

7.3.2 mfCA and mfTCA results

We applied the Sinkhorn (RAS-ipf) algorithm to scale the original data matrix \mathbf{N} into a unique bistochastic matrix \mathbf{D} , see Table 1. After 500 iterations, the resulting probability matrix $\mathbf{Q} = (q_{ij} = \frac{d_{ij}}{IJ} = \frac{d_{ij}}{589})$ has uniform row and column sums: $q_{i+} = \frac{1}{J} = 0.02380952$ and $q_{+j} = \frac{1}{I} = 0.025$.

Figures 1 and 2 display the maps from Goodman's mfCA and mfTCA of \mathbf{Q} , respectively. The mfCA map Figure 1 is challenging to interpret because CA is sensitive to outliers. In contrast, Figure 2 reveals a clear separation of:

- Summer (s) points lie on the right side of the plot
- Spring (sp) and Winter (w) points on the left side, with no clear separation between (sp) and (w) points. This is due to the fact that the bistochastic matrix \mathbf{D} has changed the *internal order structure* of the original row stochastic matrix \mathbf{N} .

(Insert Figures 1 and 2)

7.3.3 CA and TCA of the row stochastic dataset \mathbf{N}

Benzécri (1973b, pp. 18-27) emphasized the following fact: CA must be applied only to *homogenous* datasets; for compositional datasets this criterion was shown to be successful by Baxter et al. (1990). The available compositional dataset $\mathbf{N} = (n_{ij})$ being row stochastic is homogenous, that is, $\sum_j n_{ij} = 100$ for $i = 1, \dots, 42$, while the column sums vary $0.2543986 \leq \sum_i n_{ij} \leq 558.1079$. Figures 3 and 4 display the CA and TCA maps of \mathbf{N} respectively, where we clearly see the separation of the three seasonal specimens.

(Insert Figures 3 and 4)

7.4 Sacred Books dataset

Sah and Fokoué (2019) constructed an extremely sparse contingency table \mathbf{N} of size $I \times J = 590 \times 8266$. Here, 590 denotes fragments of chapters

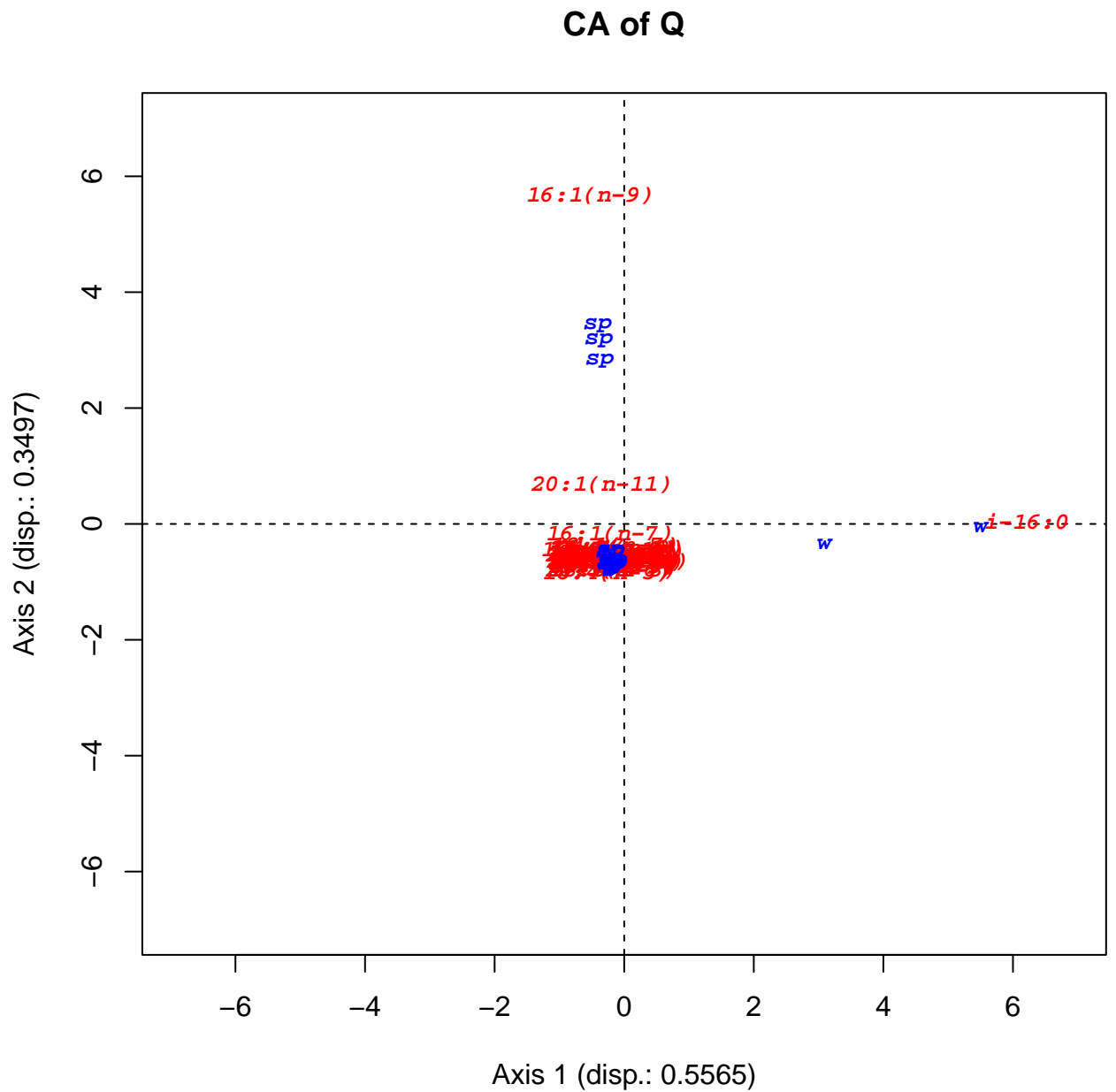


Figure 1: mfCA of Copepods dataset.

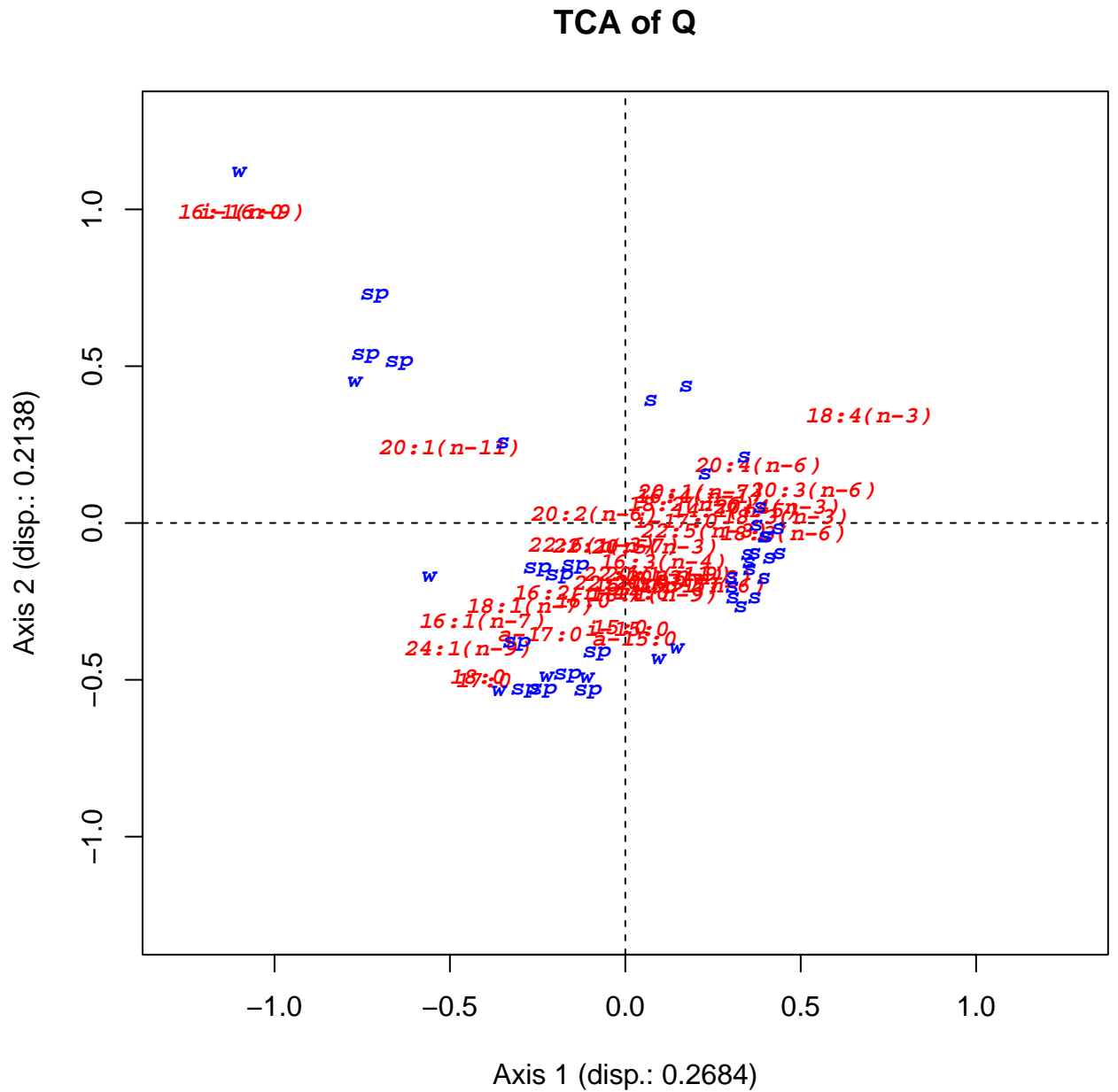


Figure 2: mfTCA of Copepods dataset.

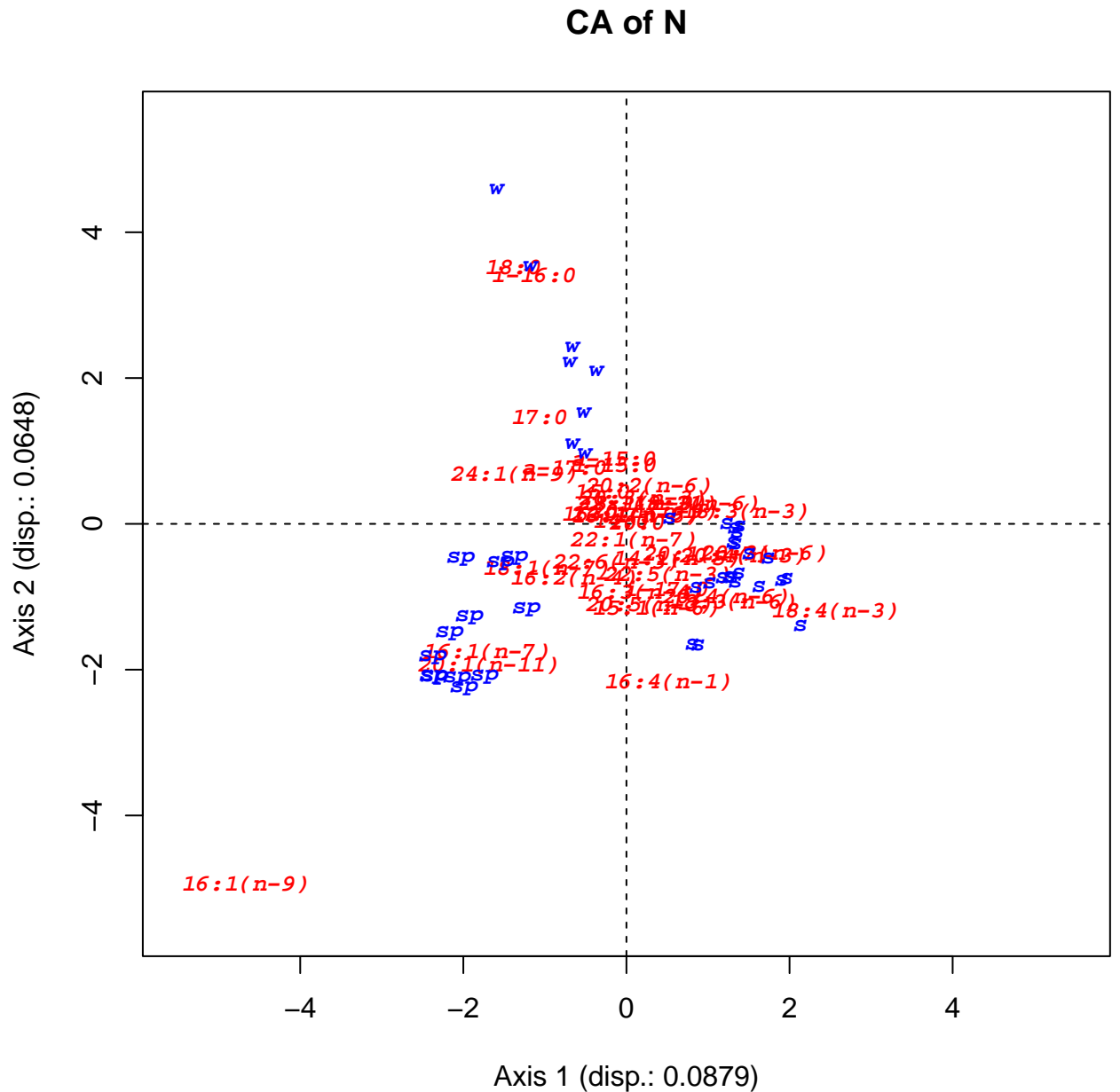


Figure 3: CA of RowStochastic Copepods dataset.

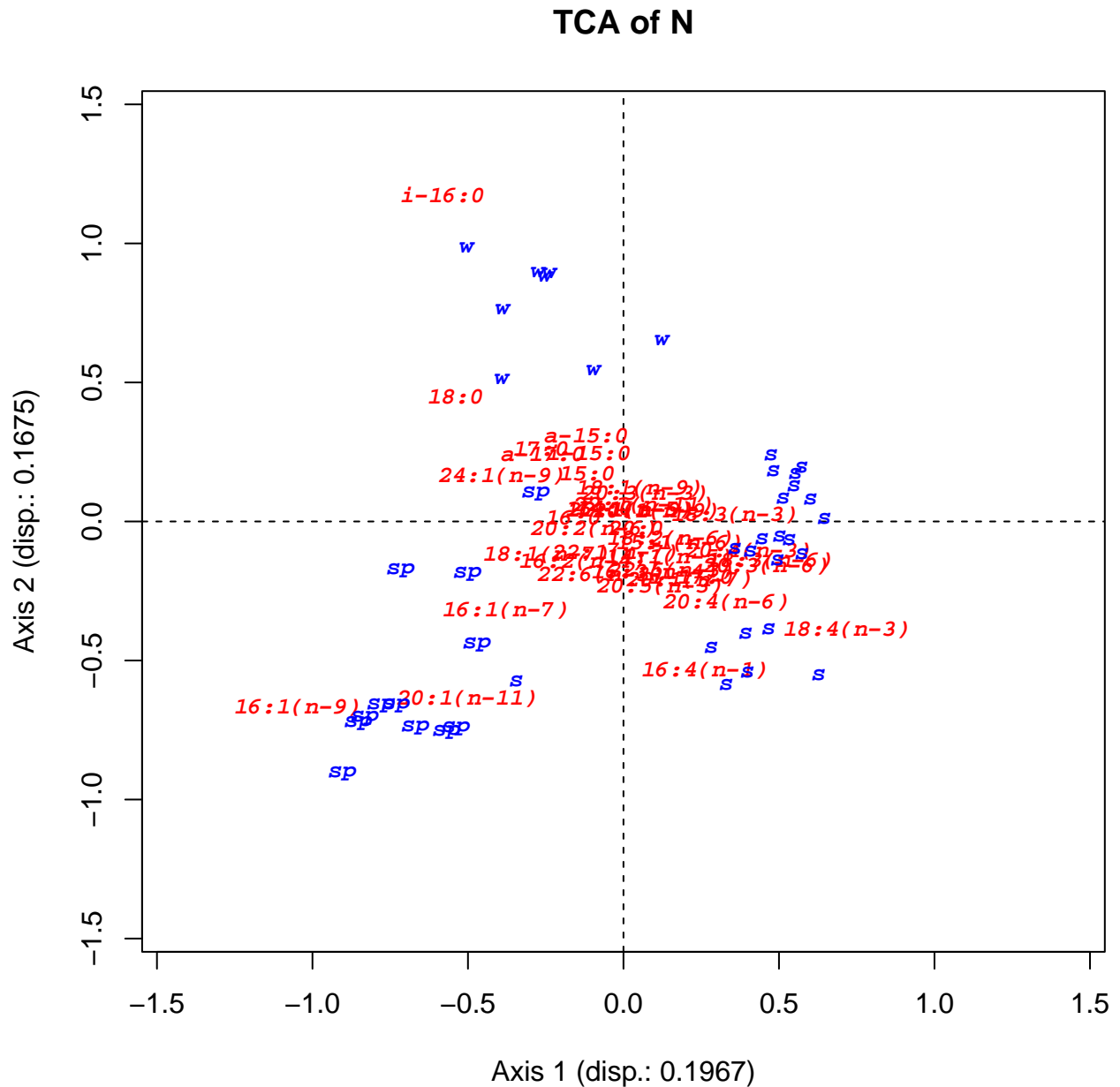


Figure 4: TCA of RowStochastic Copepods dataset.

extracted from English translations of eight sacred books, and 8 266 is the number of distinct words (tokens) across the chosen fragments.

The dataset includes fragments from four Biblical books and four extreme-Orient texts. The symbols in parentheses will label each fragment on the CA and TCA maps:

Text	Symbol	Number of chapters
Four Noble Truths of Buddhism	B	45
Tao Te Ching	T	81
Upanishads	U	162
Yogasutras	Y	189
Book of Proverbs	P	31
Book of Ecclesiastes	E	12
Book of Ecclesiasticus	e	50
Book of Wisdom	W	19

7.4.1 Sparsity and dataset characteristics

- The total number of Oriental chapters is 478, with 30 252 words counted. The total number of Biblical chapters is 112, with 30 355 words counted. So, on average, the Oriental fragments are much sparser than the Biblical ones.

- The apparent sparsity of \mathbf{N} is 99.14%. After merging and eliminating the one empty fragment (chapter 14 of the B text), we obtain the CA sparsity of $(\mathbf{N}) = \text{apparent sparsity} (\mathbf{N}_{\text{merged}}) = 98.65\%$, where $\mathbf{N}_{\text{merged}}$ is of size 589×4864 . Note that the marginal count of the words in the chosen fragment of chapter 14 of the B book is null; so in CA and TCA this row is eliminated. This extreme sparsity (often described as high dimensionality) poses challenges for many analysis methods.

7.4.2 Dimension-reduction methods reviewed by Ma, Sun & Zou (2023)

Ma, Sun and Zou visualized the dataset with twelve classic methods and their newly proposed meta-visualization method:

- 1) Principal component analysis (PCA) (Hotelling 1933)
- 2) Multi-dimensional scaling (MDS) (Torgerson 1952)
- 3) Non-metric MDS (iMDS) (Kruskal 1964)
- 4) Sammon's mapping (Sammon) (Sammon 1969)
- 5) Kernel PCA (kPCA) (Scholkopf, Smola and Muller 1998)
- 6) Locally linear embedding (LLE) (Roweis and Saul 2000)

- 7) Isomap (Tenenbaum, Silva and Langford 2000)
- 8) Hessian LLE (HLLE) (Donoho and Grimes 2003)
- 9) Laplacian eigenmap (LEIM) (Belkin and Niyogi 2003)
- 10) t-SNE (van der Maaten and Hinton 2008)
- 11) Uniform manifold approximation and projection for dimension reduction (UMAP) (McInnes, Healy and Melville 2018)
- 12) Potential of Heat-diffusion for Affinity-based Trajectory Embedding (PHATE) (Moon et al. 2019)
- 13) Meta-visualization (meta-spec) (Ma, Sun and Zou 2022, 2023)

7.4.3 CA and TCA of the count compositional dataset \mathbf{N}

When analyzing the dataset \mathbf{N} , two interpretations arise:

- If \mathbf{N} represents the full population of all sacred-text chapter-fragments, CA's use of actual marginal weights accurately reflects sacred-texts structure.
- If \mathbf{N} is viewed as a count compositional sample (akin to the Cups, rodent and Copepods datasets), scale-invariant CA methods are more appropriate. Given that the contingency table is extremely sparse, we can have three variants:

a) Figures 5 and 6 display the CA and TCA maps of $\text{sign}(\mathbf{N})$ for the 589 fragments. The CA map is difficult to interpret, while the TCA map closely resembles the PHATE and Meta-Spec visualizations, clearly separating Biblical fragments (left) from Oriental fragments (right).

(Insert Figures 5 & 6 here)

b) Figure 7 represents the TCA map of Benzécri's homogenous row stochastic transformed dataset $\text{RS}(\mathbf{N})$, where we clearly note the dominance of the Oriental fragments (distributed in three quadrants) over the Biblical fragments (concentrated in one quarter) due to the fact that number of Oriental chapters is 478, while the number of Biblical chapters is 112.

(Insert Figure 7 here)

c) Figure 8 represents row stochastic transformed dataset $\text{RS}(\text{sign}(\mathbf{N}))$, where we clearly note its close similarity with Figure 7, with the only difference is the change of positions of the 44 B points.

(Insert Figure 8 here)

7.4.4 mfCA limitations

Table 4 presents the final ten iterations of the Sinkhorn (RAS-ipf) algorithm applied to \mathbf{N} . Although the algorithm converges to two solutions—similar to the rodent dataset in Table 1—the iteration at step 1499 in Table 4

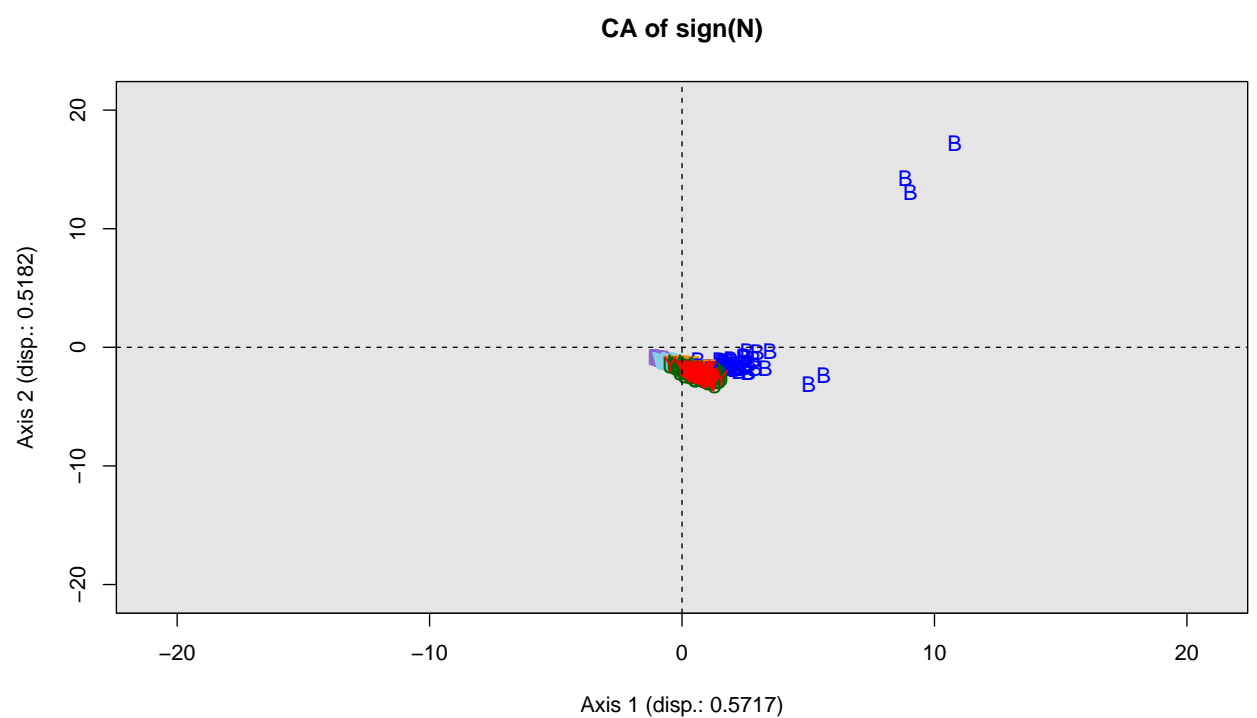


Figure 5: CA of $\text{sign}(\text{SacredBooks})$ dataset.

TCA of sign(N)

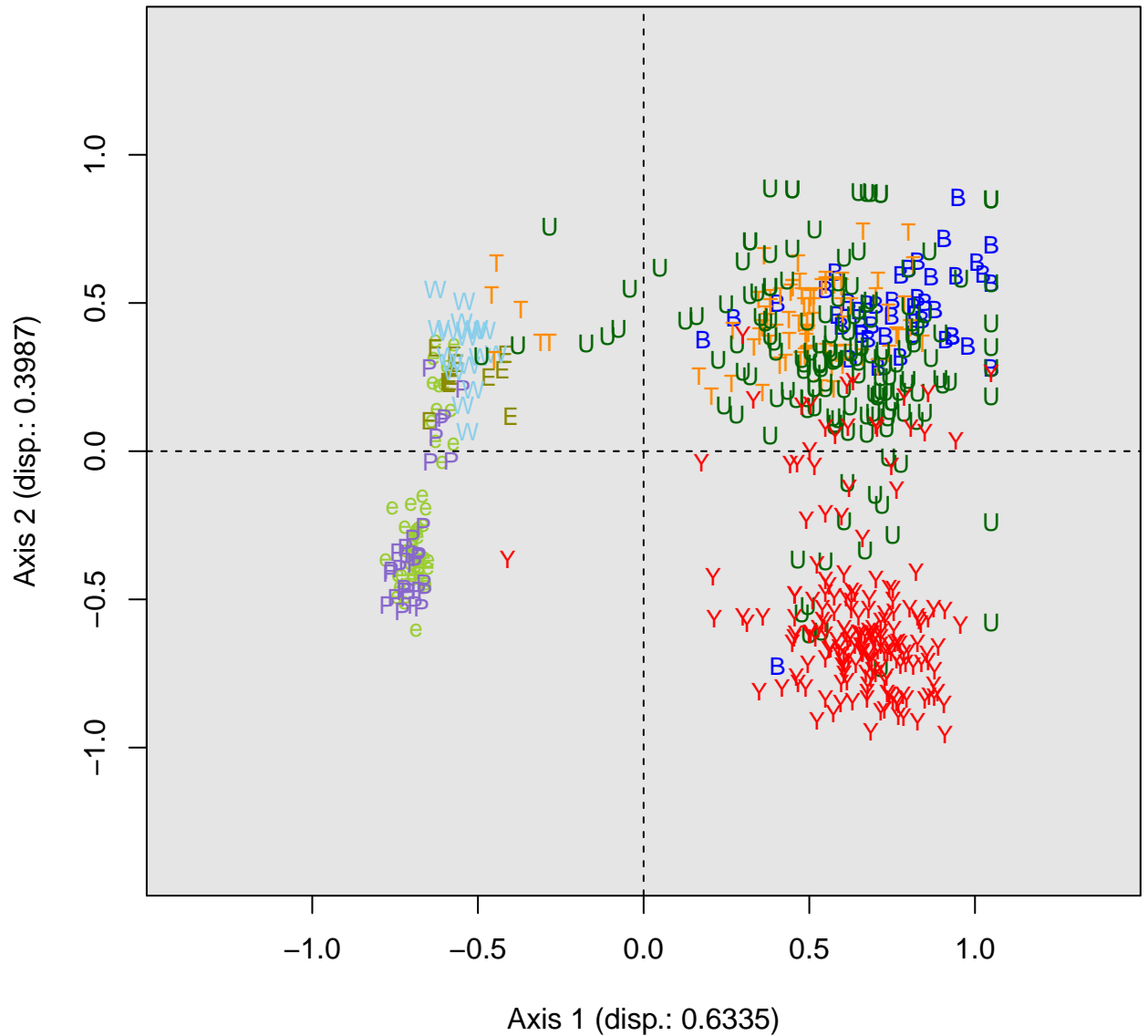


Figure 6: TCA of sign(SacredBooks) dataset.

TCA of RowStoch(N)

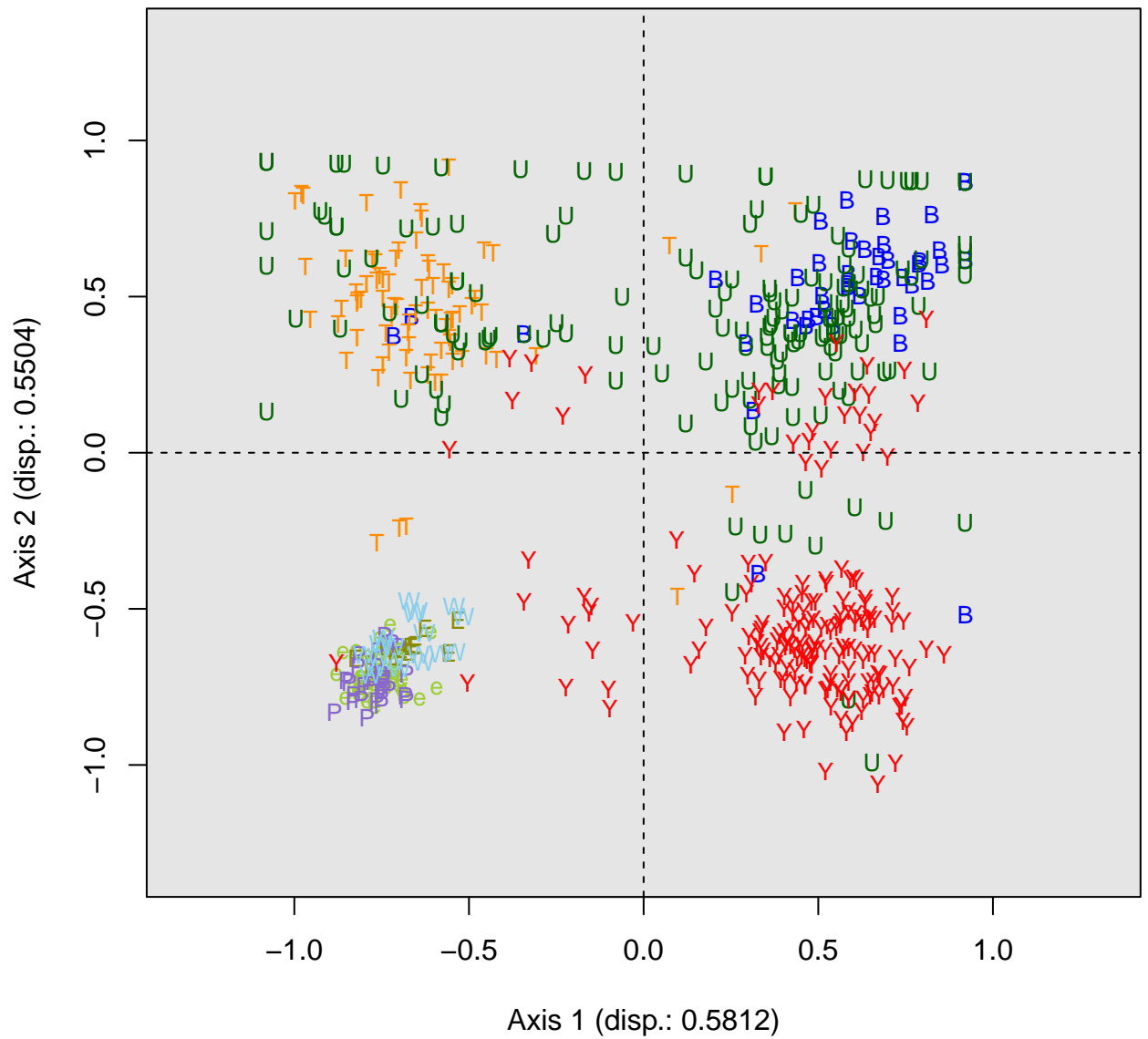


Figure 7: TCA of RowStochastic (Sacred Books) dataset.

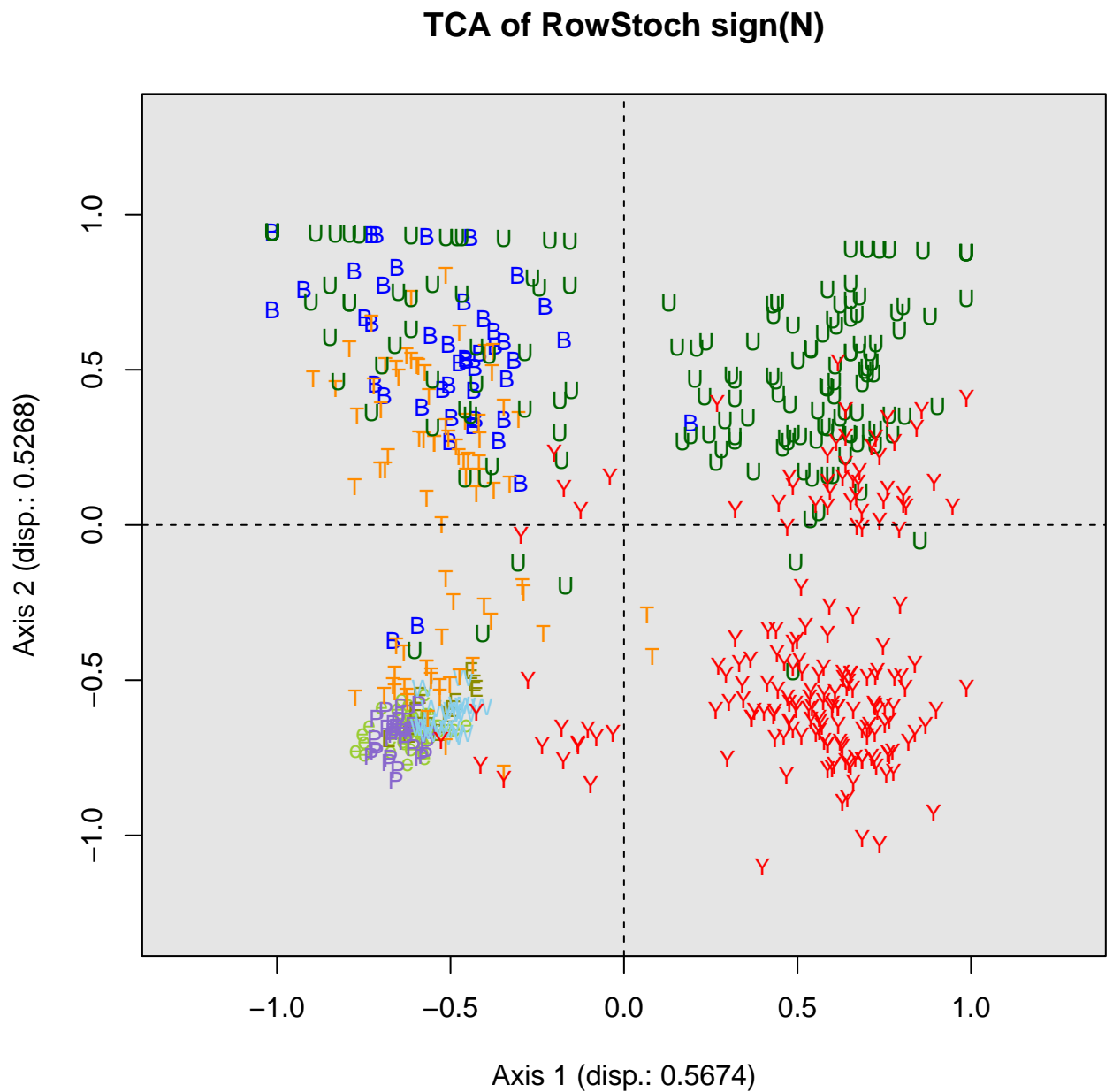


Figure 8: TCA of RowStochastic sign(Sacred Books) dataset.

yields $C2_{dist} = 1793232$, indicating at least 111 diagonal blocks in the underlying structure, see Appendix. This enormous value demonstrates that both mfCA and mfTCA struggle with extremely sparse datasets and are therefore not recommended here.

Table 4: Sinkhorn (RAS-ipf) algorithm iteration results.

<i>Sacred Books</i>		
<i>iteration</i>	$C2_{dist}$	<i>ratio</i>
1491	1.793233e+06	1.002523
1492	1.855228e+06	1.002523
1493	1.793233e+06	1.002523
1494	1.855228e+06	1.002523
1495	1.793233e+06	1.002523
1496	1.855228e+06	1.002523
1497	1.793232e+06	1.00253
1498	1.855227e+06	1.002523
1499	1.793232e+06	1.002523
1500	1.855227e+06	1.002523

8 Conclusion

We conclude our exploration by summarizing three key takeaways:

First, we analyzed four datasets of varying sparsity using three scale-invariant CA methods and one row stochastic CA method. For each dataset, we selected the combination of methods best suited to its sparsity level.

Dataset	Sparsity %	Methods applied
Cups (nonsparse)	0	Greenacre & Goodman
Copepods (moderately sparse)	11.69 (adjusted)	Goodman & RS
Rodents (sparse)	68.48 (adjusted)	sign-transform & RS
Sacred Books (extremely sparse)	98.65% (CA-sparsity)	sign-transform & RS

Second, applying the Sinkhorn (RAS-ipf) algorithm to a nonnegative dataset may alter its internal order structure, thereby emphasizing the local micro-level structure in Goodman's mfCA approach.

Third, by applying both CA and TCA side by side, we:

- Capture complementary dimensions of association in contingency tables and compositional data

- Enhance robustness to sparsity and extreme values

- Provide richer visualization and interpretation for exploratory analysis

Overall, combining the three scale-invariant CA/TCA variants and one row stochastic CATCA method offers a versatile toolkit for uncovering structure across compositional datasets from nonsparse to extremely sparse.

Declarations

Funding: Partial funding to Choulakian is provided by the Natural Sciences and Engineering Research of Canada (Grant no. RGPIN-2017-05092).

Data availability: The four real datasets used in this paper are available online.

References

- Aitchison J (1986) *The Statistical Analysis of Compositional Data*. London: Chapman and Hall
- Allard J, Choulakian V (2019) *Package TaxicabCA in R*. Available at: <https://CRAN.R-project.org/package=TaxicabCA>
- Baxter MJ, Cool HM and Heyworth MP (1990) Principal component and correspondence analysis of compositional data: some similarities. *Journal of Applied Statistics* 17, 229–235
- Beh E, Lombardo R (2014) *Correspondence Analysis: Theory, Practice and New Strategies*. N.Y: Wiley
- Belkin M, Niyogi P (2003). Laplacian eigenmaps for dimensionality reduction and data representation. *Neural Computation*, 15 (6), 1373-1396
- Benzécri JP (1973a) *L'Analyse des Données: Vol. 1: La Taxinomie*. Paris: Dunod
- Benzécri JP (1973b) *L'Analyse des Données: Vol. 2: L'Analyse des Correspondances*. Paris: Dunod
- Bolger DT, Alberts AC, Sauvajot RM, Potenza P, McCalvin C, Tran D, Mazzoni S, Soule M (1997) Response of rodents to habitat fragmentation on coastal southern California. *Ecological Applications*, 7, 552–563
- Brualdi RA, Parter SV, Schneider H (966) The diagonal equivalence of a nonnegative matrix to a stochastic matrix. *Journal of Mathematical Analysis and Applications*, 16, 31–50
- Choulakian V (2006) Taxicab correspondence analysis. *Psychometrika*, 71, 333-345
- Choulakian V (2016) Matrix factorizations based on induced norms. *Statistics, Optimization and Information Computing*, 4, 1-14
- Choulakian V (2017) Taxicab correspondence analysis of sparse contingency tables. *Italian Journal of Applied Statistics*, 29 (2-3), 153-179
- Choulakian V (2023) Notes on correspondence analysis of power transformed data sets. <https://arxiv.org/pdf/2301.01364.pdf>
- Choulakian V, Allard J, Mahdi S (2023) Taxicab correspondence analysis and Taxicab logratio analysis: A comparison on contingency tables and

- compositional data. *Austrian Journal of Statistics*, 52, 39 – 70
- Choulakian V, Mahdi S (2024) Correspondence analysis with prespecified marginals and Goodman's marginal-free correspondence analysis. In Beh, Lombardo, Clavel (eds): Analysis of Categorical Data from Historical Perspectives: Essays in Honour of Shizuhiko Nishisato, pp 335–352, Springer
- Cuadras CM, Cuadras D, Greenacre M (2006) A comparison of different methods for representing categorical data. *Communications in Statistics - Simulation and Computation*, 35(2), 447-459
- Donoho DL, Grimes C (2003). Hessian eigenmaps: Locally linear embedding techniques for high-dimensional data. *Proceedings of the National Academy of Sciences*, 100 (10), 5591-5596
- Gifi, A. (1990). Nonlinear Multivariate Analysis. Wiley, New York
- Goodman LA (1991) Measures, models, and graphical displays in the analysis of cross-classified data. *Journal of the American Statistical Association*, 86 (4), 1085-1111
- Goodman LA (1996) A single general method for the analysis of cross-classified data: Reconciliation and synthesis of some methods of Pearson, Yule, and Fisher, and also some methods of correspondence analysis and association analysis. *Journal of the American Statistical Association*, 91, 408-428
- Graeve M, Greenacre M (2020) The selection and analysis of fatty acid ratios: A new approach for the univariate and multivariate analysis of fatty acid trophic markers in marine pelagic organisms. *Limnology and Oceanography: Methods*, 18(5), 183-195
- Greenacre M (1984) *Theory and Applications of Correspondence Analysis*. Academic Press
- Greenacre M (2009) Power transformations in correspondence analysis. *Computational Statistics & Data Analysis*, 53(8), 3107-3116
- Greenacre M (2010) Log-ratio analysis is a limiting case of correspondence analysis. *Mathematical Geosciences*, 42, 129-134
- Greenacre M (2020) *R package easyCODA*. Available at:
<https://CRAN.R-project.org/package=easyCODA>
- Greenacre M (2024). The chiPower transformation: a valid alternative to logratio transformations in compositional data analysis. *Adv Data Anal Classif* 18, 769–796. <https://doi.org/10.1007/s11634-024-00600-x>
- Greenacre M, Lewi P (2009) Distributional equivalence and subcompositional coherence in the analysis of compositional data, contingency tables and ratio-scale measurements. *Journal of Classification*, 26, 29-54
- Greenacre M, Nenadic O, Friendly M (2022) *R Packa ca*. Available at:
<https://CRAN.R-project.org/package=ca>

- Hotelling H (1933) Analysis of a complex of statistical variables into principal components. *Journal of Educational Psychology*, 24(6), 417-441
- Idel M (2016) A review of matrix scaling and Sinkhorn's normal form for matrices and positive maps. <https://arxiv.org/pdf/1609.06349.pdf>
- Kruskal JB (1964) Nonmetric multidimensional scaling: A numerical method. *Psychometrika*, 29 (2), 115-129
- Landa B, Zhang T, Kluger Y (2022) Biwhitening reveals the rank of a count matrix. *SIAM J Math Data Sci*, 4(4):1420-1446. Also available at: <https://arxiv.org/pdf/2103.13840.pdf>
- Le Roux B, Rouanet H (2004) *Geometric Data Analysis*. Springer NY
- Lewi PJ (1976) Spectral mapping, a technique for classifying biological activity profiles of chemical compounds. *Arzneim Forsch (Drug Res)*, 26:1295-1300
- Loukaki M (2023) Doubly stochastic arrays with small support. *Australasian Journal Of Combinatorics*, 86(1) 136–148
- Ma R, Sun E, Zou J (2023) A spectral method for assessing and combining multiple data visualizations. *Nat Commun* 14, 780 <https://doi.org/10.1038/s41467-023-36492-2>. Available also at: <https://arxiv.org/pdf/2210.13711>
- Madre JL (1980) Méthodes d'ajustement d'un tableau à des marges. Cahiers de l'analyse des données 5(1) 87-99, <http://eudml.org/doc/87981>. Madre (1980)
- Marshall AW, Olkin I, Arnold BC (2009) *Inequalities: Theory of Majorization and Its Applications*. Springer NY
- McInnes L, Healy J, Melville J (2018). Umap: Uniform manifold approximation and projection for dimension reduction. [arXiv:1802.03426](https://arxiv.org/abs/1802.03426)
- Moon KR, van Dijk D, Wang Z, Gigante S, Burkhardt DB, Chen WS, Yim K, van den Elzen A, Hirn MJ, Coifman RR, Ivanova NB, Wolf G, Krishnaswamy S (2019). Visualizing structure and transitions in highdimensional biological data. *Nature Biotechnology* 37 (12), 1482-1492
- Murtagh F (2005) *Correspondence Analysis And Data Coding With Java And R*. Taylor & Francis, UK
- Quinn G, Keough M (2002) *Experimental Design and Data Analysis for Biologists*. Cambridge University Press, Cambridge, UK
- Rao CR (1973) *Linear Statistical Inference and Its Applications*. John Wiley and Sons: NY
- Roweis ST, Saul LK (2000) Nonlinear dimensionality reduction by locally linear embedding. *Science*, 290 (5500), 2323-2326
- Sammon JW (1969) A nonlinear mapping for data structure analysis. *IEEE Transactions on Computers*, 100 (5), 401-409

- Scholkopf B, Smola A, Muller KR (1997) Kernel principal component analysis. In *International Conference on Artificial Neural Networks*, 583-588, Springer
- Sinkhorn R (1964) A relationship between arbitrary positive matrices and doubly stochastic matrices. *Ann. Math. Statist.* 35, 876-879
- Sinkhorn R, Knopp P (1967) Concerning nonnegative matrices and doubly stochastic matrices. *Pacific J. Math.*, 21(2):343–348, 1967. URL: <https://projecteuclid.org:443/euclid.pjm/1102992505>
- Tenenbaum JB, Silva V, Langford JC (2000) A global geometric framework for nonlinear dimensionality reduction. *Science*, 290 (5500), 2319-2323
- Torgerson W (1952) Multidimensional scaling: I. theory and method. *Psychometrika*, 17(4), 401–419
- Tsagris M, Preston S, Wood A (2011) A data-based power transformation for compositional data. In *4th International Workshop on Compositional Data Analysis*, J.J. Egozcue, R. Tolosana-Delgado, and M.I. Ortego, eds., Girona, Spain. International Center for Numerical Methods in Engineering (CIMNE) Barcelona, Spain, 2011, pp. 1–8. Available at <http://hdl.handle.net/2117/366618>
- Tsagris M, Alenazi A, Stewart C (2023) Flexible non-parametric regression models for compositional response data with zeros. *Statistics and Computing*, 33, 1-17. Available at <https://doi.org/10.1007/s11222-023-10277-5>, 106
- Tukey JW (1977) *Exploratory Data Analysis*. Addison-Wesley: Reading, Massachusetts
- Yule GU (1912) On the methods of measuring association between two attributes. *JRSS*, 75, 579-642
- van der Maaten L, Hinton G (2008) Visualizing data using t-SNE. *Journal of Machine Learning Research* 9(Nov), 2579-2605
- Ward K, Macfarlane G (020) *Package ipfr in R*. Available at:
<https://CRAN.R-project.org/package=ipfr>

Appendix

```
iteration = 1500 or 1499    ca(dij)$sv
[1] 1.0000000 1.0000000 1.0000000 1.0000000 1.0000000 1.0000000 1.0000000
1.0000000
[9] 1.0000000 1.0000000 1.0000000 1.0000000 1.0000000 1.0000000 1.0000000
1.0000000
[17] 1.0000000 1.0000000 1.0000000 1.0000000 1.0000000 1.0000000 1.0000000
1.0000000
```

[25] 1.0000000 1.0000000 1.0000000 1.0000000 1.0000000 1.0000000
 1.0000000
 [33] 1.0000000 1.0000000 1.0000000 1.0000000 1.0000000 1.0000000
 1.0000000
 [41] 1.0000000 1.0000000 1.0000000 1.0000000 1.0000000 1.0000000
 1.0000000
 [49] 1.0000000 1.0000000 1.0000000 1.0000000 1.0000000 1.0000000
 1.0000000
 [57] 1.0000000 1.0000000 1.0000000 1.0000000 1.0000000 1.0000000
 1.0000000
 [65] 1.0000000 1.0000000 1.0000000 1.0000000 1.0000000 1.0000000
 1.0000000
 [73] 1.0000000 1.0000000 1.0000000 1.0000000 1.0000000 1.0000000
 1.0000000
 [81] 1.0000000 1.0000000 1.0000000 1.0000000 1.0000000 1.0000000
 1.0000000
 [89] 1.0000000 1.0000000 1.0000000 1.0000000 1.0000000 1.0000000
 1.0000000
 [97] 1.0000000 1.0000000 1.0000000 1.0000000 1.0000000 1.0000000
 1.0000000
 [105] 1.0000000 1.0000000 1.0000000 1.0000000 1.0000000 0.9999999
 0.9999999
 [113] 0.9999998 0.9999998 0.9999998 0.9999996 0.9999994 0.9999994 0.9999987
 0.9999982
 [121] 0.9999976 0.9999973 0.9999971 0.9999949 0.9999940 0.9999933 0.9999916
 0.9999907
 [129] 0.9999879 0.9999860 0.9999857 0.9999830 0.9999829 0.9999744 0.9999565
 0.9999042
 [137] 0.9998845 0.9998704 0.9998388 0.9998303 0.9998243 0.9998098 0.9998003
 0.9997900
 [145] 0.9997572 0.9997502 0.9997118 0.9997023 0.9997001 0.9996577 0.9995629
 0.9995457
 [153] 0.9995050 0.9994306 0.9993534 0.9993510 0.9993496 0.9993461 0.9993224
 0.9993088
 [161] 0.9993075 0.9992959 0.9992790 0.9992493 0.9992439 0.9992186 0.9992142
 0.9992085
 [169] 0.9992076 0.9991986 0.9991561 0.9990049 0.9989804 0.9989786 0.9989749
 0.9989159
 [177] 0.9989024 0.9987829 0.9987727 0.9987690 0.9987292 0.9986991 0.9984546
 0.9984065

[185] 0.9984009 0.9983052 0.9981344 0.9981019 0.9980984 0.9980983 0.9980219
 0.9979210
 [193] 0.9978944 0.9978376 0.9978274 0.9977364 0.9977316 0.9977285 0.9977223
 0.9976919
 [201] 0.9976404 0.9976010 0.9975551 0.9975516 0.9974197 0.9973882 0.9973433
 0.9973228
 [209] 0.9971855 0.9969870 0.9969393 0.9968935 0.9968566 0.9967788 0.9967049
 0.9966357
 [217] 0.9964829 0.9964476 0.9963342 0.9962191 0.9961630 0.9961446 0.9960815
 0.9958977
 [225] 0.9958652 0.9958554 0.9957947 0.9957758 0.9957730 0.9957716 0.9957323
 0.9956531
 [233] 0.9955773 0.9952718 0.9952445 0.9951317 0.9951046 0.9949589 0.9948421
 0.9948358
 [241] 0.9946760 0.9946431 0.9943875 0.9942713 0.9941642 0.9940914 0.9940410
 0.9940356
 [249] 0.9939414 0.9937308 0.9935095 0.9933060 0.9932102 0.9931092 0.9930615
 0.9929306
 [257] 0.9928601 0.9928295 0.9925974 0.9925626 0.9924373 0.9922767 0.9922610
 0.9922431
 [265] 0.9920729 0.9920425 0.9919547 0.9918366 0.9918350 0.9917942 0.9915453
 0.9914892
 [273] 0.9911905 0.9911121 0.9909367 0.9908857 0.9907796 0.9906793 0.9906354
 0.9906282
 [281] 0.9905022 0.9904279 0.9904134 0.9903917 0.9903752 0.9903060 0.9900805
 0.9899054
 [289] 0.9898829 0.9897441 0.9897386 0.9895356 0.9895161 0.9893045 0.9892339
 0.9891573
 [297] 0.9890011 0.9889965 0.9888289 0.9888264 0.9887329 0.9885884 0.9884499
 0.9884249
 [305] 0.9883281 0.9880578 0.9879792 0.9878656 0.9877138 0.9876940 0.9875869
 0.9873000
 [313] 0.9872883 0.9872604 0.9871252 0.9870861 0.9867917 0.9867712 0.9867281
 0.9863939
 [321] 0.9861168 0.9860737 0.9859532 0.9857569 0.9857475 0.9857252 0.9856825
 0.9854015
 [329] 0.9852575 0.9851506 0.9849342 0.9847880 0.9846818 0.9846278 0.9845084
 0.9844634
 [337] 0.9843424 0.9842373 0.9835844 0.9833021 0.9832924 0.9829480 0.9829328
 0.9829049

[345] 0.9828540 0.9826716 0.9825560 0.9825123 0.9824157 0.9822316 0.9821151
 0.9820461
 [353] 0.9819228 0.9818451 0.9813221 0.9813052 0.9810376 0.9810045 0.9809847
 0.9805979
 [361] 0.9805581 0.9803791 0.9800348 0.9797959 0.9792255 0.9789450 0.9789224
 0.9788074
 [369] 0.9785766 0.9784028 0.9783570 0.9781365 0.9779832 0.9779813 0.9779671
 0.9779209
 [377] 0.9778849 0.9775773 0.9774715 0.9773847 0.9772981 0.9772069 0.9771841
 0.9770516
 [385] 0.9767973 0.9767793 0.9767718 0.9763481 0.9762838 0.9755859 0.9755749
 0.9755571
 [393] 0.9753048 0.9753038 0.9751698 0.9751271 0.9749917 0.9745571 0.9745226
 0.9744746
 [401] 0.9743928 0.9743431 0.9742835 0.9741217 0.9738488 0.9735054 0.9733233
 0.9727307
 [409] 0.9726781 0.9724381 0.9723704 0.9723146 0.9720727 0.9718992 0.9712859
 0.9712407
 [417] 0.9711802 0.9705660 0.9705552 0.9704082 0.9702667 0.9698933 0.9698900
 0.9692294
 [425] 0.9688700 0.9684887 0.9682634 0.9682319 0.9679514 0.9676946 0.9675131
 0.9669772
 [433] 0.9668160 0.9667117 0.9666040 0.9663994 0.9662453 0.9660918 0.9659918
 0.9657493
 [441] 0.9656911 0.9656375 0.9649920 0.9644599 0.9644458 0.9643957 0.9642596
 0.9642332
 [449] 0.9640634 0.9636526 0.9636256 0.9633100 0.9631252 0.9631247 0.9627706
 0.9627315
 [457] 0.9625069 0.9624609 0.9622236 0.9617261 0.9616493 0.9609082 0.9608423
 0.9607209
 [465] 0.9606808 0.9602031 0.9601826 0.9598969 0.9595925 0.9592491 0.9590916
 0.9587804
 [473] 0.9583899 0.9580232 0.9577250 0.9567925 0.9564024 0.9561637 0.9560063
 0.9560031
 [481] 0.9559409 0.9555687 0.9550438 0.9548637 0.9548146 0.9547520 0.9533340
 0.9530938
 [489] 0.9528115 0.9527882 0.9517189 0.9511896 0.9508099 0.9506287 0.9502582
 0.9494205
 [497] 0.9494071 0.9487999 0.9487477 0.9486811 0.9474266 0.9471492 0.9466498
 0.9464657

[505] 0.9463625 0.9460308 0.9460213 0.9459221 0.9455041 0.9449110 0.9439099
 0.9435329
 [513] 0.9434508 0.9434305 0.9432871 0.9428326 0.9426490 0.9420296 0.9412092
 0.9411211
 [521] 0.9394350 0.9388870 0.9380430 0.9376750 0.9372849 0.9366966 0.9358015
 0.9357109
 [529] 0.9350730 0.9345864 0.9337436 0.9330633 0.9299461 0.9295742 0.9293285
 0.9290859
 [537] 0.9280448 0.9278056 0.9269726 0.9257694 0.9257612 0.9251830 0.9244718
 0.9240081
 [545] 0.9239780 0.9239617 0.9215778 0.9215532 0.9205492 0.9205181 0.9194363
 0.9161280
 [553] 0.9149813 0.9148949 0.9139334 0.9105601 0.9095867 0.9068417 0.9055099
 0.9014791
 [561] 0.9006996 0.8992565 0.8975730 0.8956672 0.8938989 0.8914348 0.8865637
 0.87666786
 [569] 0.8766368 0.8722169 0.8708924 0.8683782 0.8653681 0.8551611 0.8551513
 0.8411667
 [577] 0.8364237 0.8306574 0.8167284 0.8102990 0.8078165 0.7959309 0.7813042
 0.7049943
 [585] 0.6749376 0.5941499 0.4983027 0.3236741